Scientific African 8 (2020) e00359

Contents lists available at ScienceDirect

Scientific African

journal homepage: www.elsevier.com/locate/sciaf

# Robust crystalline silicon photovoltaic module (c-Si PVM) for the tropical climate: Future facing the technology[☆]

Frank K.A. Nyarko[a,*], G. Takyi[a], Emeka H. Amalu[b,*]

[a] Mechanical Engineering Department, College of Engineering, Kwame Nkrumah University of Science and Technology Kumasi, Ghana
[b] Department of Engineering, School of Science and Engineering and Design, Teesside University, Middlesbrough, Tees Valley, TS1 3BA, UK

ARTICLE INFO

*Article history:*
Received 12 July 2019
Revised 20 February 2020
Accepted 18 March 2020

*Keywords:*
Crystalline silicon photovoltaic module
Elevated ambient temperature
Interconnection failure
Module life span

ABSTRACT

A critical impediment to the adoption and sustained deployment of crystalline silicon photovoltaic modules (c-Si PVMs) in the tropical climate is the accelerated degradation of their interconnections. At 40.7% c-Si PVM interconnect failure rate worldwide and significantly higher in the tropics. A review of impact of elevated ambient temperature operations on accelerated interconnection degradation is critical to achieving the system's sustainability and reliability up to the 25-year design lifespan. This study reviews critical module's operational parameters to advise on the future facing creation of robust module for the tropical region. Key areas reviewed include manufacturing process, solar cell efficiency, interconnection technology and R&D parameters. The review discusses the state-of-the-art in c-Si PVM interconnection technologies and propose back-junction-back-contact (BJ-BC) cell technology for adoption in the manufacture of the next generation of robust c-Si PVM for the tropics. The review findings provide insight into the future facing the robust c-Si PVM technology that is useful to the module design engineers.



## Introduction

The warranty period of c-Si solar photovoltaic (SPV) modules has increased rapidly and significantly in recent years. At present, the goal of the PV industry is to develop photovoltaic system that can attain a thirty-year service life [60,75,76,132]. Realisation of this length of service is possible when the rate of power degradation of the modules per year is between 0.5% and 1.0% maximum. However, [38,63,126] have reported that installed modules experience annual power degradation rate of about 0.5% to 10%. A number of factors cause c-Si SPV installed in the field to degrade. A key factor is the exposure to a range of cyclic temperatures coupled with elevated temperature operations. Cyclic thermal loading induces thermo-mechanical fatigue damage in the solder joints in c-Si SPV module interconnects. Operations under a range of currents and voltages play a significant role in accumulating power degradation in the SPV modules. The band-gap of ultra violet (UV) light incident on the SPV cells impacts on the degradation rate. Huge variation in weather conditions also significantly increase the degra-

☆ Editor name:

* Corresponding author.
*E-mail addresses:* fnyarko.coe@knust.edu.gh (F.K.A. Nyarko), E.Amalu@tees.ac.uk (E.H. Amalu).

https://doi.org/10.1016/j.sciaf.2020.e00359

dation rate. The cumulative contributions of these factors on the degradation of SPV operating in tropical climate is critical. Macben et al. [89] demonstrated that the degradation and failure mechanisms of SPV are location dependent. Other factors associated with packaging material, interconnection, solder joint, adhesion, delamination, moisture accumulation and semiconductor device thermal challenges degrade module performance and reduce its power output, which increase SPV reliability concerns.

PV modules installed in hot and humid climate experience significant increase in moisture accumulation. Moisture is found to diffuse into the module via backsheets and the encapsulant that is ethylene vinyl acetate (EVA). Moisture penetration weakens the adhesive bonds within the laminated interfaces. The occurrence leads to delamination and loss of passivation [95]. Moisture intrusion corrodes the solder joints in c-Si PV module [37,54,105]. Investigations by Köntges et al. [74] show that significant losses in PV module performance are caused by corrosion of cell from the Si-$N_x$ anti-reflection coating (ARC), or the corrosion of metallic materials such as solder bonds and Silver fingers. Presently, there are no industry standard methods to determine long-term photovoltaic module performance in the field. However, infant mortality failures of PV modules can be determined using industry standard certification tests as suggested in [61,135]. This is a useful tool to identify critical module design and manufacture parameters. The IEC 61215 thermal cycling test standard requires that PV modules are subjected to 200 cycles from -40 °C to 85 °CC. Modules that record above 5% relative power degradation is deemed to have failed the test. As reported by Meydbray et al. [92], PV modules cannot be subjected to 30 year outdoor tests for every design iteration. Therefore, accelerated laboratory test to failure testing (TFT) on identified failure mechanisms must be used to assess long-term effect on module output power. There is considerable activity right now in the PV industry [11,45,128,133] to develop various methodologies and models to predict the service life of installed SPV modules.

Understanding degradation mechanisms in PV modules is a crucial step in attempting to mitigate degradation rate. King et al. [70] reported that field modules experience temperature swings of about 60 °C (maximum) each day. The temperature swings culminate in initiation and development of fatigue cracks in the solder interconnection. This is occasioned by mismatch of the co-efficients of thermal expansion (CTE) of silicon, glass, copper and solder bonded together. The CTE mismatch can be local and global. Kardjilov et al. [26] explained that global CTE mismatch results when solder joints are stresssed and deformed to accommodate the effect of CTE mismatch from surrounding component materials which include cells, glass and interconnect. Similarly, local CTE mismatch results when the expansion of solder material is restricted or enhanced by the material it is soldered to. One effect of solder joint degradation is the formation of micro-cracks. Crack may propagate across the entire joint area - resulting in an open circuit. An open circuit increases the electrical resistance across the solder joint. In turn, this phonomenon significantly impact on c-Si PVM output power. High current PV modules are largely affected because power loss is associated with increasing series resistance ($R_s$) in the form $I^2R_s$ [2,136].

Solder creeps when its temperature increases. The creep response is significant at high homologous temperatures that characterise tropical climate [130]. Creep in solder is associated with grain boundary sliding (GBS) and matrix creep (MC). The latter has been observed to have a more damaging creep mechanism which leads to a shorter joint life. Kardjilov et al. [26] also observed that creep mechanism is both temperature and stress dependent and increases with increase in strain rate/deformation. A consequence of soldered tin-containing interconnection in c-Si PVM is formation of brittle intermetallic compound (IMC) layer. The IMC layer are formed between the solder and the copper ribbon interface on one side and the solder and silver fingers on the other side. The IMC is basically $Cu_3Sn_5$ or $Ag_3Sn$ grains suspended in a solder matrix. During thermal cycling of the PV module, the resulting thermo-mechanical stress leads to a change in the microstructure of the IMC layer in the solder joint (coarsening and thickening). This layer is therefore subseptible to crack initiation and propagation. The effect is critical for elevated temperature operations.

In solar PV systems, the incident radiations outside the useful bandgap which is not converted into electrical energy is transformed into thermal energy. The generated thermal energy increases the temperature of the PV module which accelerates the thermo-mechanical degradation of the interconnection. The life of a PV module largely depends on the reliability of the interconnection technology used in its design and manufacture [141]. To ensure reliable supply of energy, these properties must be maintained during the entire service life of the PV module. Thus, management of the thermal energy is very important to realise the c-Si SPV module 25-year designed life-span for tropical operations.

A robust c-Si PVM for the tropical climate can be realised through critical review of factors affecting module performace in elevated temperature climates. These factors are associated with solar cell power conversion efficiency and thermo-mechanical reliability of solder joint interconnections in the module. The review will provide new kowledge on thermal effects of these factors for improved c-Si PV module design.

## Manufacturing, interconnection technology and reliability of c-Si PVM

Efficient design of robust c-Si PVM for the tropics demands that effective manufacturing technique and process be adopted. It is also imperative that factors affecting solar cell efficiency and power output be designed for. The integrity of solder interconnection in c-Si PVM impacts both the power conversion efficiency (PCE) and power output (PO). Therefore, the knowledge of the operations of silicon solar cell and thermo-mechanical response of the interconnection are vital in its effective design. This section presents and discusses the manufacturing processes, efficiency, interconnection technology and reliability.

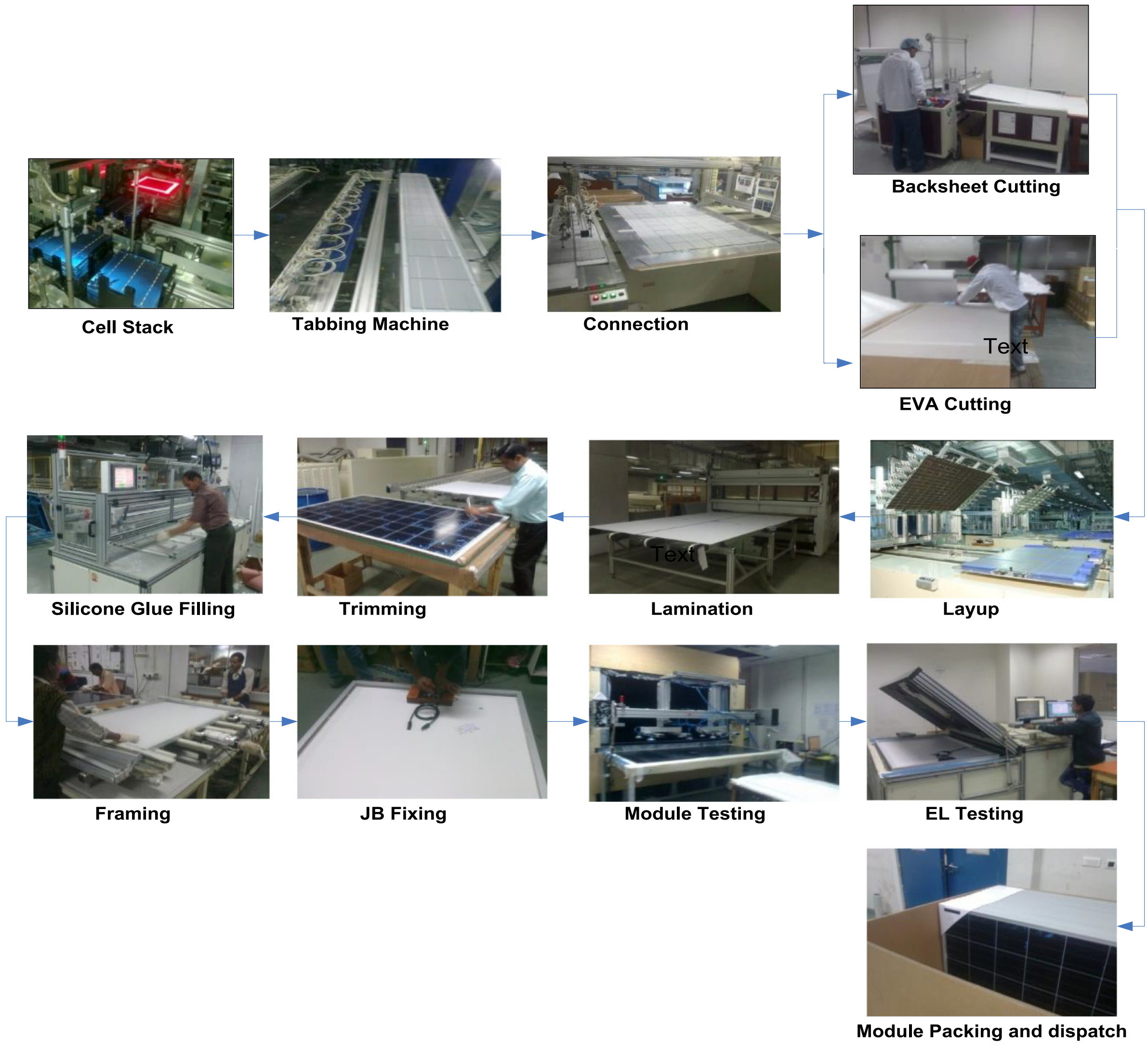


**Fig. 1.** The assembly process flow of c-Si PV-module.

Assembly and manufacturing processes

Fig. 1 shows an assembly process of c-Si PV module. Sorted cells of defined efficiency band are stacked to minimise mismatch issues. The cells are usually of the same colour class. Quality check is performed to identify front and back visual defects. Cells are interconnected in a stringing and tabbing process per power requirement. The stringed cells are checked to ensure there is no cell breakage or chipping. A further check is conducted to ensure that cell to cell gap and the pull strength (>2 Newton) of ribbons on front and back bus bars are implemented. A backsheet of appropriate dimension with no contamination on either side is cut as well as the front and back Ethylene Vinyl Acetate (EVA) encapsulant. The strings are connected using string connectors and fixed EVA tapes.

The correct position of the EVA fixing tape and the right placement and directions of strings are ensured. Generally, the layup sequence involves: Glass-Front EVA – connected strings – Back EVA – Back Sheet. Dark current-voltage (IV) characteristic curves are taken to correct faults at interconnections before lamination. An electroluminescence (EL) of the cell strings are also verified in the process. Defects associated with this assembly process include: black cell, dry solder, broken cell, shorted string and wrong interconnection.

Lamination process is the main crystallizing step in the PV-module assembly. Lamination protects the module from the harsh environmental conditions. It is expected to endure throughout the module's service life. Thus, a reliable module lamination is critical in ensuring that cells attain their designed life. The lamination process is proceeded by a gel test - performed to determine the insoluble fraction of curved EVA. The gel test is expected to yield 75% of cross linked material. A peel test of over 40 N magnitude between Glass to EVA and EVA to back sheet is conducted. Poor lamination could lead to

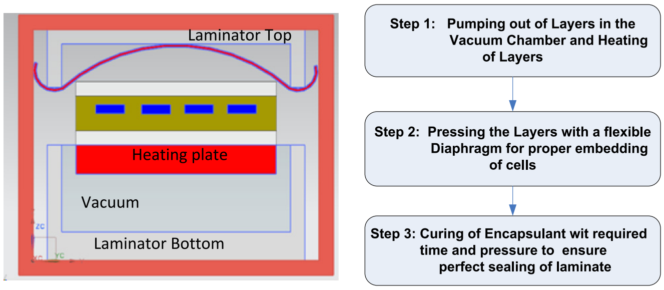


**Fig 2.** c-Si PV module lamination process.

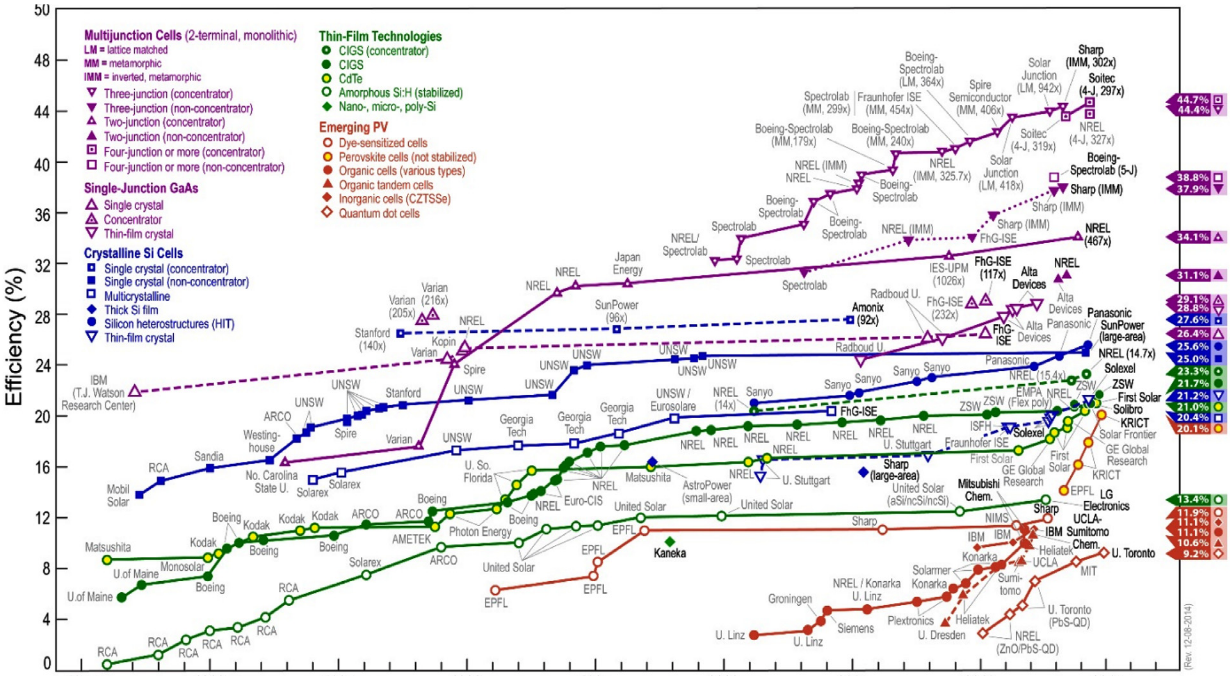


**Fig. 3.** Best research solar cell efficiencies reported by NREL (© NREL 2015).

delamination of EVA from edges or inside the module. Delamination leads to corrosion of the cells during exposure to the environment. Poor lamination traps air bubbles inside the module. The occurrence leads to cell corrosion. Poor gel content (<75% of cross linked material) leads to gradual seepage of moisture into the module which culminates in cell corrosion. The lamination process consists of three main steps. These are shown in Fig. 2. After lamination, excess EVA and backsheet protruding from the glass is trimmed before module is framed. Framing process involves pressing silicone filled short and long frames with all sides of the laminated edges such that the laminate is uniformly covered. The junction box is then fixed and the module is ready for electrical safety testing.

Modules are tested for safety before it becomes market ready. The tests include: insulation, high pot (test for high voltage insulation), wet leakage and ground continuity. Flash test is performed to check the current-voltage (IV) characteristics of the module. A final quality assurance of EL (Electroluminescence) test - for identification of any defects (cracks in the cells) is performed to certify the module for packaging and dispatch.

The production of c-Si PV module spans over half a century – accounting for its largest production share. It has up to 90% production share of all solar cell produced [115,116]. Silicon material is abundant in nature and represents over 26% of the Earth's crustal material with very negligible environmental impact [116]. Silicon solar cells remain dominant in the PV industry. Fig. 3 presents '*Best research solar cell efficiencies as reported by NREL*'. The Figure shows that c-Si cells provide high-energy conversion efficiencies compared to other commercial solar cells and modules. Its efficiency is about 27.6%. Significant increase in installation of solar PV in the tropical ambient is projected by the year 2020.

The c-Si PV cell is poised as the most viable option to meet this demand because it is the most suitable for large scale production [112].

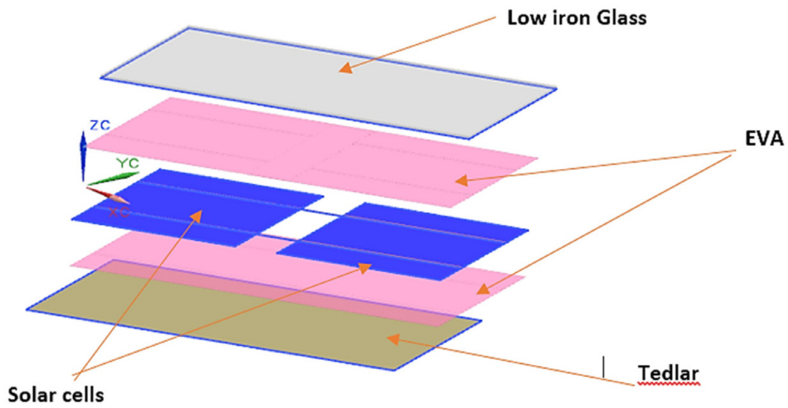


**Fig. 4.** Exploded view of a typical solar PV-module.

In general, solar cells are manufactured from thin wafer discs with thickness of about 200 µm [71]. The various manufacturing steps involved in the production of silicon cells include; etching, coating, screen printing and firing. Conventional solar cells have metallization grid on the front side, which collects the light generated charge. This grid is connected to busbars. Current is transferred through the PV-module from one cell to another by means of flat copper ribbons soldered to the busbars. The copper ribbons provide a conduit for current transfer from one cell to a neighbouring cell in a series interconnection referred to a strings. A typical solar PV-module is made up of a transparent cover glass with anti-reflective coating (ARC), an encapsulant made from ethylene vinyl acetate (EVA), a rear support layer of tedlar material, a frame and a junction box with connecting cables as schematically represented in Fig. 4. The module provides mechanical support to the crystalline silicon solar cell as well as protection to the electrical interconnections from harsh environmental conditions. The PV-module is heamatically sealed to prevent water or water vapour from corroding the electrical contacts.

Various components of the PV module play important and unique roles during the module manufacturing as well as operation in the field. A solar cell should possess good solderable pads with no printing defects or micro-cracks. The EVA encapsulant must be optically transparent (360 nm minimum) with low thermal resistance. It must also offer a firm adhesion between solar cells. The tedlar backsheet should exhibit high thermal resistance and low moisture permeability. The glass cover (with ARC) must not trap air bubbles or have chipping at the edges. The junction box (JB) houses the by-pass diodes and connecting cables. A typical JB can take any of the following configurations (IP X(Y));

- IP 65- total protection against dust ingress, low pressure water jets from any direction permitting a limited ingress of water.
- IP 67- total protection against dust ingress, short periods of water exposure.

A 1.6 $\times$ 0.23 mm ribbon and a 5 $\times$ 0.22 mm string bus connector are the two main types of interconnect ribbons used in assembling solar cells. A connecting ribbon has a copper core with solder coating on the top and bottom side. A typical PV solder coating thickness is approximately (25 $\pm$ 10) µm. The backbone of the module structure consists of short and long anodized Aluminum frames. The frames have perforations (holes). Each perforation has specific functionality. There are installation holes used for fixing modules to various structures. It contains drain holes used to drain water from rain and melting snow. There are also ground symbols with holes, which is for grounding the module. It has holes in the hollow part of the frame which primarily provide ventilation to keep module at uniform temperature.

## Interconnection technology and reliability

The performance of a PV module is hugely affected by the interconnection technology used to connect the cells. In response to the miniaturization manufacturing trend, coupled with the drive for cheaper PV module, there has been steady reduction in the thickness of silicon wafers in solar PV module.

Recently wafer thickness of below 200 micron are being used in the manufacture of solar cells [71]. The reduction in wafer thickness is expected to continue to values below 100 µm [94,117,118]. [44] have argued that thinner cells may lead to cost reduction and increased module performance. However, the reliability of such fragile cells remains a major concern [117]. Currently, cell interconnection technique commonly used in the industry involves IR (infrared) soldering of copper ribbons to form strings of interconnection between separate cells. This procedure usually leads to formation of micro-cracks on the wafer (especially for long strings of thin cells). This is a challenging reliability concern for PV modules. The IR soldering technique, which produces a continuous line of solder, induces a high mechanical stress in the soldered joint resulting in accelerated fatigue damage in the soldered joint. A selective laser soldering technique where a number of single solder spots [7-8 spots evenly distributed on each busbar (Fig. 5)] are applied on the copper ribbons mitigates the situation.

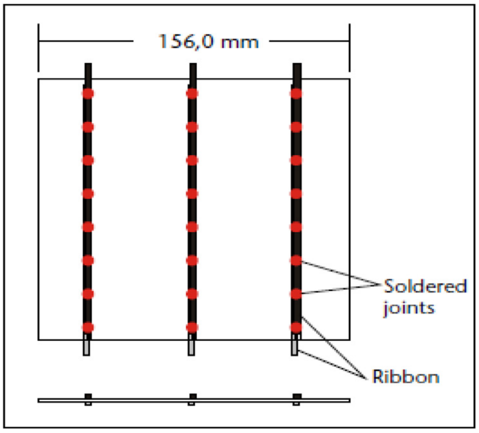


**Fig. 5.** Selective laser soldering of a 3-busbar solar cell [143].

Selective laser soldering has been reported to induce minimal mechanical damage to the soldered joint, with a potential to improve production yield [143].

Simultaneous stringing and tabbing process where soldering is done on the front and back metallization of the cell results in a single thermal cycle. The resulting balancing effect of the front and back surfaces reduces the bow experienced by the wafer. Reducing shadowing losses by reducing the width of the copper ribbons remains a research concern. With reduced wafer thickness, wafer breakage during stringing and tabbing process is also expected to rise. Usually, a reliable solder joint is achieved with good solder wettability of the surface. Good substrate wettability ensures good adhesion to the soldered component [123]. For solar cells, the soldered components consist of two metals (Silver (Ag) from the cell busbar and Copper (Cu) from interconnection). Theoretically, solder joint failure is registered in three main locations. These are at the copper interconnect/solder; at the silver busbar/solder and within the solder itself. It is reported that the dominant failure sites are the Ag/solder interface as well as within the solder itself [28,62]. The main cause of failure at these sites are the mismatch of coefficient of thermal expansion (CTE) of the bonded materials. The influence of interconnection technology on the performance and long-term power degradation is very critical in PV module design. Interconnects are expected to be designed to minimize global CTE mismatch induced stress on the solder joint while keeping electrical resistance at the minimum [16]. The next section discusses various cell interconnection technologies currently used in the manufacture of SPV modules.

## State-of-the-art in c-Si PV module interconnection technologies

Several interconnection technologies are employed in the design and manufacture of c-Si PV module. In this section, two key technologies (conventional front-to-back cell and back-contact solar cell interconnections) are presented and discussed. The section presents further information on the configurations of back-contact solar cell design.

### Conventional front-to-back cell interconnection technology

Fig. 6 displays schematically the architecture of conventional front-to-back cell interconnection technology.

The configuration consists of a front metal electrode and back contacts on the cell material. A solder-coated copper ribbon with high electrical conductivity is connected along the top face of a cell and soldered to the back of a neighbouring cell. This interconnection ensures current transfer across respective cells in a series connection [71]. The configuration has metallization which enables it to interface with two different materials - the Si wafer and the solder-coated Cu ribbon. In solar cells electrons are generated and transferred from the Si wafer to the Ag metal fingers. The contact between silicon wafer and the silver finger must therefore be of a higher integrity for efficient electron transfer [31]. Silver fingers are deposited on the silicon wafer by a screen printing technique that generates an unbroken H-pattern of narrow and tall fingers connected by wider busbars. In order to minimise optical losses, the Ag metal fingers must have a large aspect ratio (narrow and tall). This also maximizes the cross-sectional area for increased conductivity [24,97].

Front side screen-printing results in unbroken H-pattern of narrow fingers connected by wider busbars. This process enables optimized system production. This process is succeeded by baking out the solvent and then firing the cell at elevated temperatures of about 4800 °C - forming both front and rear contacts simultaneously [31]. The conventional front-to-back interconnection geometry introduces a kink in the copper ribbons as they connect the back to the front side. This geometric distortion induces stresses in the copper ribbons during manufacture, which is aggravated further by high thermal loading during operation in tropical ambient temperatures. The findings from degradation studies of many field-aged PV modules with this interconnect technology [7,21,41,131] report the claim. The cell interconnection technology remains dominant in

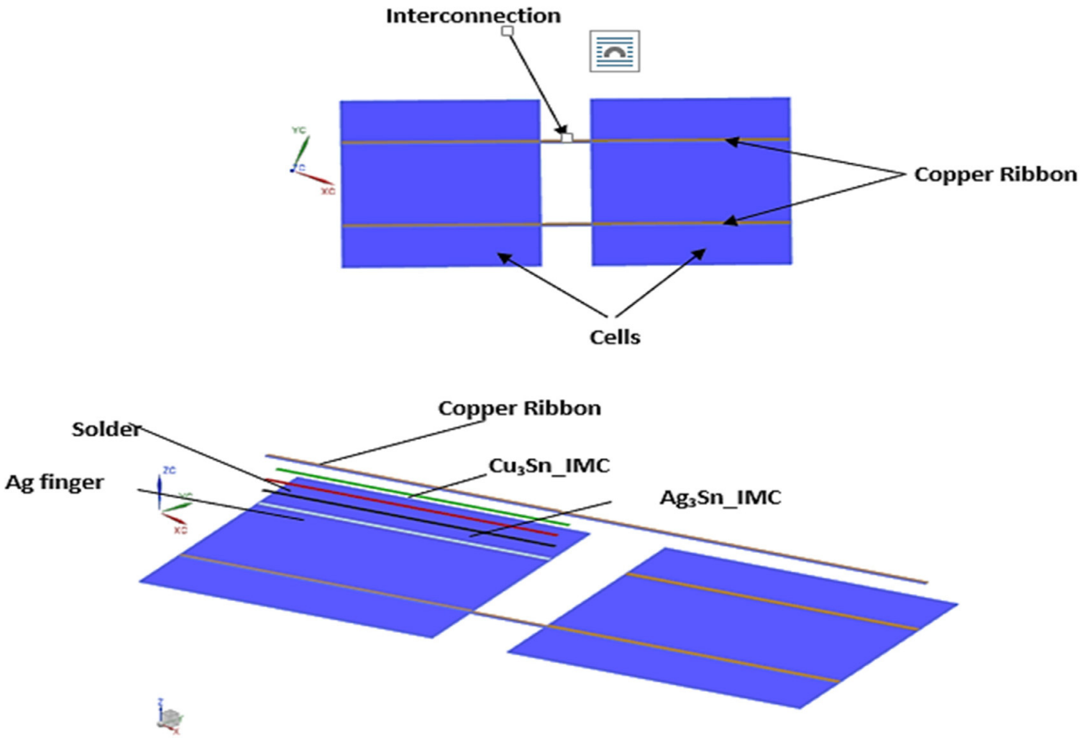


**Fig. 6.** Conventional front-to-back cell interconnection technology.

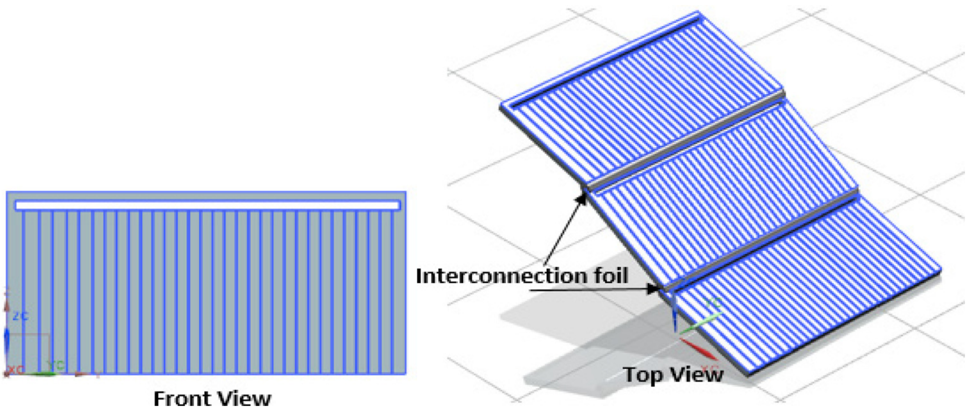


**Fig. 7.** Schematic drawing of a cell for shingled cells interconnection.

the PV industry. However, new interconnection schemes are emerging which show significant departure from the conventional structure. Current research reports of interconnection based on parallel Cu wires known as the Smartwire [42] or Multibusbars approaches [15] where a conventional full area Al BSF and standard screen printing for the front contact have been used for a 6" Cz-Si multi-busbar solar cells and efficiencies of up to 19.5% recorded. The interconnection technique is gaining a lot of attention because they enable higher cell efficiency (through lower shading) and lower cost as a result of lower Ag consumption for the fingers which can be very thin. Efficient mini-modules with little silver consumption and with or without copper based metallization has been demonstrated by Faes et al. [1]. The new mini-modules continues to show promising results.

An emerging interconnection technique known as 'shingled cell interconnection' (shown in Fig 7), where narrow cells are arranged in a manner that each cell overlaps a little with the other is currently under research and development. In this architecture, the busbars are connected back-to-front through a joint material. This structure yields high efficient modules because there are no shading losses due to busbars or ribbons, and the active area is close to 100% of the total area [8].

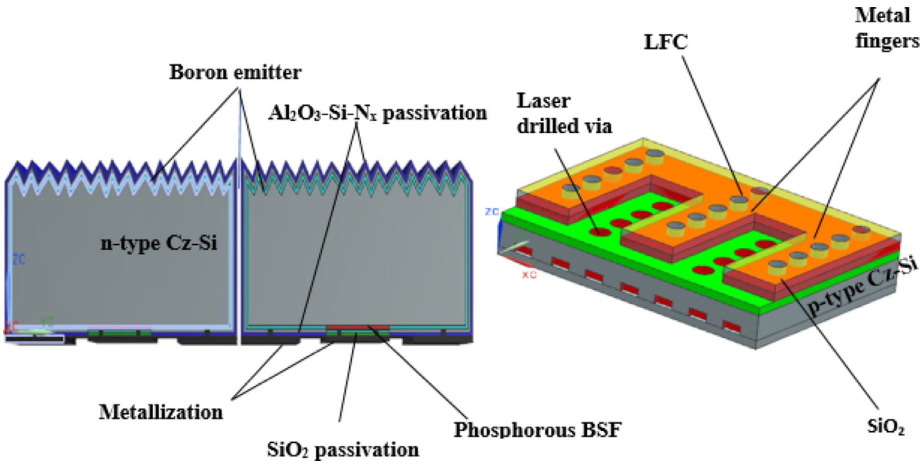


**Fig. 8.** Schematic cross section of the EWT solar cell.

Back-contact (BC) solar cell interconnection technologies

The back-contact (BC) solar cells require unique interconnection design. In a conventional interdigitated back-contacted solar cells (IBC), the rear sides of neighbouring cells are joined. This contrasts with conventional solar cells that the front sides are joined with the rear sides of neighbouring cells. The BC interconnect design has gridless front surface which improves light trapping and passivation. Charge recombination losses are also eliminated since all contacts appear at the rear of the cell.

There are several configurations of BC cells which include the following:

i EWT (Emitter Wrap Through).
ii Metallization Wrap Through (MWT).
iii Back-Junction back-contact (BJBC).
iv Alternate p-and n-type.
v Pin-up modules (PUM).
vi Silver solar cells.
vii Spherical solar cell.
viii Cells with electrode wire grid (Day 4 Electrode).

The subsequent sub-sections present and discuss the various BC architectures listed above.

*Emitter Wrapped Through (EWT) cell interconnection*

The architecture of EWT cell is such that it allows photocurrent to be collected by both the front and back surface connected in parallel by a multiplicity of small-area interconnection paths [67]. The configuration enables the performance of EWT cell to be over a wide range and nearly independent of the cell thickness to diffusion length ratio [82].The vias are formed by photolithographic patterning and etching indentations that do not penetrate [84] or barely penetrate [53] through the wafer. The prevailing front surface diffusion reduces any limitation posed by contact size and spacing up to the levels attained in screen-printing. However, according to Eikelboom et al. [39], theoretically deduced optimal pattern is difficult to achieve within the accuracy of screen printed technology. Gee et al. [46] therefore propose the buried contact cell technology for EWT cell design since formation of the groves and vias can be done in a single step which in-turn ensures a good alignment. It is reported that the technology has recorded cell efficiencies up to 21.4% on small areas (6 $cm^2$) [124]. EWT cells has relatively low diffusion length to cell thickness ratio. However, screen-printed large EWT cells have high series resistance which limits the size factor. The schematic cross-section of the EWT solar cell technology is shown in Fig. 8.

The metallization involved in creating cell interconnection of EWT show a linear pattern of metal fingers. Induced stresses from manufacturing of these metal fingers are generally low compared with front-to-back cell interconnection. Additionally, the metallization is somewhat 'shielded' from direct incidence of thermal radiation due to her position in the cell architecture. EWT cell interconnects are therefore expected to register relatively lower induced thermo-mechanical stresses from elevated ambient temperatures.

*Metallization Wrap Through (MWT) cell interconnection*

The metallization wrap through (MWT) back-contact cell interconnection is achieved by the use of a flexible printed circuit board (PCB). The respective cells are interconnected only at the back sides since the terminals for both base and emitter are placed on the back sides by design. The interconnection which is a flexible PCB therefore replaces the copper ribbons in the traditional assembly.

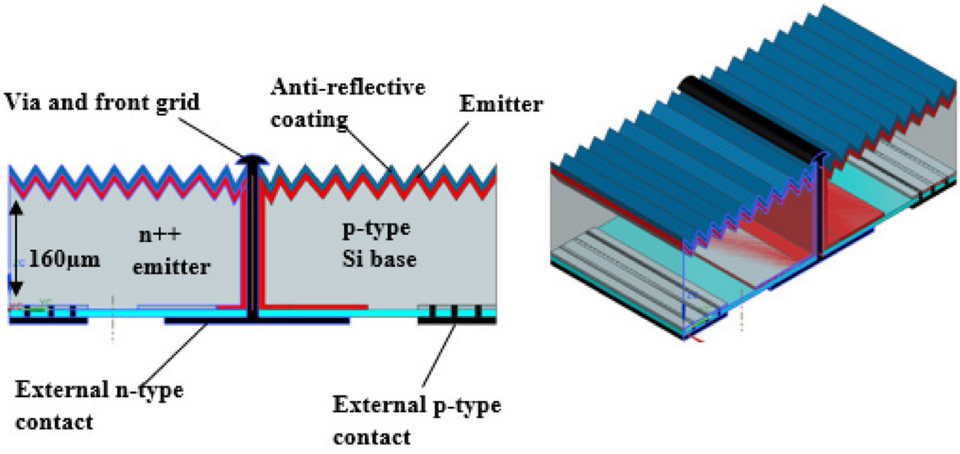


**Fig. 9.** MWT cell interconnection.

The flexible PCB interconnect is less susceptible to induced thermo-mechanical damage from elevated temperatures compared with the conventional H-patterned interconnect. This is because the interconnect technique involved in connecting the respective cells yields a comparatively lower manufacturing induced stress. This cell design does not eliminate front shading losses since there is presence of a metal grid on the front surface in combination with interconnection pads for both polarities on the rear surface [67]. However, by placing the interconnection pads and solder strips at the rear, these losses are reduced significantly. Conventional H-pattern solar cells with screen printed contacts typically show approximately 7% front side shading. By applying the MWT concept, this value is reduced to 4.1% as no busbars are present on the front side [129]. Unlike EWT the surface termination of the space charge region in MWT cells are limited in length. This situation can be mitigated by restricting the emitter to the front surface and the metal contact separated from the silicon by a thick metal insulator on its way to and on the rear surface as shown in Fig 9. The Fig 9 presents the schematic of cross section of MWT cell interconnection.

According to Kerschaver and Beaucarne [67], the rear surface pads can optimally be combined with extended contacted emitter region at the rear of the cell. In such configuration, the rear pads are not restricted to interconnection as their only functionality. Lamers et al. [83] reported of some MWT solar cells that have initial superior energy yield compared with conventional solar cells. Cell efficiencies higher than 17% from c-Si [58] and higher than 20% for cz-Si [86] has been achieved. The performance increase is obtained by reducing the front shadowing as a result of the back connection of the electrical contacts. This particular contact scheme ensures also the reduction of the production process costs by a reduction of the silver mass per cell [56]. The presence of vias in the junction of MWT cell structure renders it sensitive to reverse bias current. The 'through' hole metallization pattern has also been observed to promote the formation of hot spots on cell surface.

*Back-Junction back-contact (BJBC) interconnection*

The back-junction and back-contact (BJBC) solar cell architecture features an interdigitated finger structure and busbar that collects the current from individual fingers [125]. The $p^+$ and $n^+$ junctions are situated on the rear side of the device. Metallization pattern on the front surface is virtually absent and therefore there is no feature present on the surface to shadow the incident photon flux [67]. In addition, a low series resistance of the metal pattern is achieved as the metallization can cover about one half of the back surface. Unlike front-contacted cells, current conduction in BJBC cells is not through the emitter and therefore there is no trade-off between grid shading and series resistance losses. Thus, the rear function can be optimized in terms of the lowest saturation current only [91]. Research simulation and measurements reported show that the busbar regions of BJBC solar cells reduce the fill factor and short circuit current density [125]. Fig 10 shows a schematic drawing of *n*-type BJ-BC silicon solar cell.

The photogenerated carriers are near the surface and are expected to travel across the bulk region to the backside metal contacts to be collected. A high lifetime is thus required since, unlike EWT and MWT, there are no vias present. The lifetime measures the average distance carriers can travel to reach the backside region before recombination. The diffusion length covered by carriers in BJBC cells should be longer than the thickness of the silicon wafer in order to ensure an optimum performance of the cell. The use of a thinner wafer is therefore an advantage for a BJBC solar cell structure [52]. BJBC cells have coplanar cell interconnect geometry that ensure uniform linear expansion of metal contacts at elevated temperatures. At elevated temperatures, induced excess thermo-mechanical strain from expansion of metal contacts due to differences in their CTEs are thus minimised.

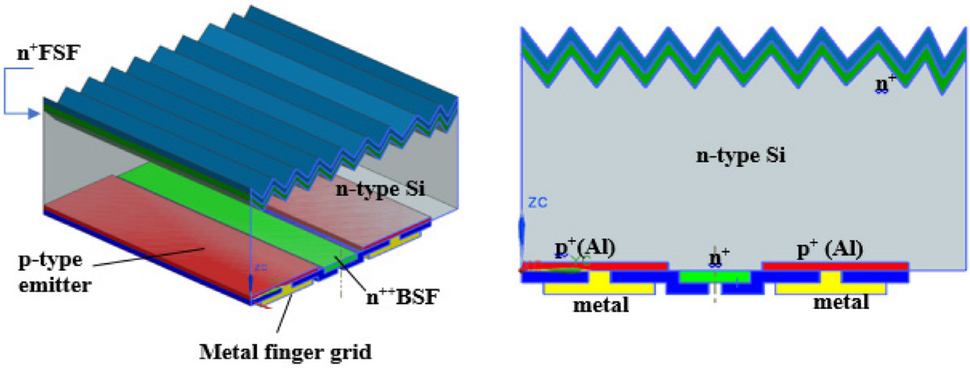


**Fig. 10.** Schematic n-type BJ-BC silicon solar cell.

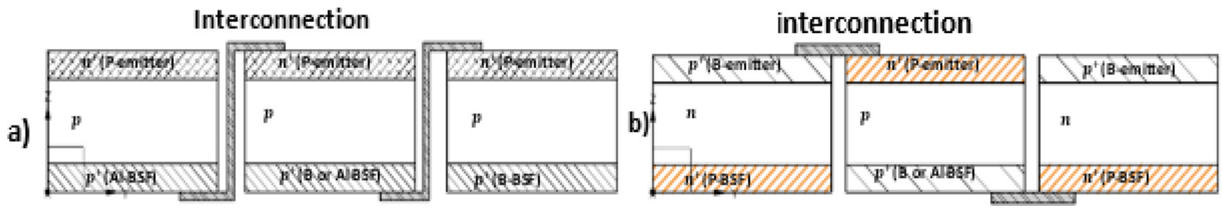


**Fig. 11.** (a) Conventional module interconnection: each cell backside is connected with the front side of the subsequent solar cell (b) Innovative interconnection using alternating p-type and n-type solar cells [16].

*Alternate p-and n-type solar cell interconnection*

Bifacial screen-printed cells are used in the construction of alternate p- and *n*-type silicon solar cells. The design deploys alternating p- and *n*-type semiconductors arranged in a manner to permit interconnection of equivalent sides on front-to-front and back-to-back of cells next to each other [16]. Investigations from Kopecek et al. [79,80] reveal that, in contrast to the p-type, the n-type is not prone to boron oxygen related light induced degradation. The schematic of the technology is shown in Fig 11.

The two solar cells have a Plasma Enhanced Chemical Vapour Deposition (PECVD) of $SiN_x$ on top of a phosphorus diffused region that serves as emitter in the case of the p-type and as a front surface field (FSF) in the n-type cell [78]. The main distinguishing feature between the p-type and n-type is the Ag-Al pad at the rear side. On the p-type interconnection the pad is directly printed on the substrate whereas on the n-type it is printed either on the $p^+$ -region or on top of Al rear contact to avoid shunting of cells [78]. The alternate p-and n-type solar cell interconnection method has a number of advantages over conventional PV-modules. These include: simpler interconnection procedure, closer assembly of cells (for aesthetic appearance) and higher yield during module fabrication. In addition to these advantages, the technology (using the bifacial cells) leads to an increase in power output as compared to standard mono-facial modules [78]. The elegant interconnect geometry that reveals a straight horizontal short-spanned connection in the alternate front-to-front and back-to-back lay-up ensures a uniform horizontal expansion of the interconnection. The arrangement eliminates any potentially high bending stresses as may be registered in the conventional H-patterned cell interconnect.

*Pin-Up Modules (PUM) interconnection*

The pin-up module (PUM) is a type of back-contact solar cells designed with a structured interconnecting back foil and limited number of holes in the wafer [145]. The holes form vias and contain pins which serve as interconnection material at the rear [17,19]. The cell has a similar geometry as a conventional cell with metallization at both front and rear sides. The only distinguishing feature with the standard cell is the presence of vias and the configuration of the interconnection. Apart from being visually more appealing than conventional modules PUM offers several performance improvements such as: reduction in shadowing losses due to the absence of busbars, reduction in resistance losses as current is collected at holes equally spaced over the wafer and good alignment during screen printing of metal contacts [138]. The schematic of PUM cell interconnection is shown in Fig 12.

The interconnection is achieved by means of a metal foil produced to specification [20]. There are several interconnection methods utilised in PUM. They include: manual soldering, localised infrared soldering, ultrasonic bonding, dispensing of conductive adhesives and thermal arc spraying [19]. The two most popular methods of this technology are the localised infrared soldering and the thermal arc spraying technique. Usually, the localised infrared soldering is preferred over the other as the soldering area at the front of the cell is relatively small. In thermal arc spraying a metal powder is sprayed onto the surface of a foil and subsequently into vias in the cell. The interconnection realised is further laminated with

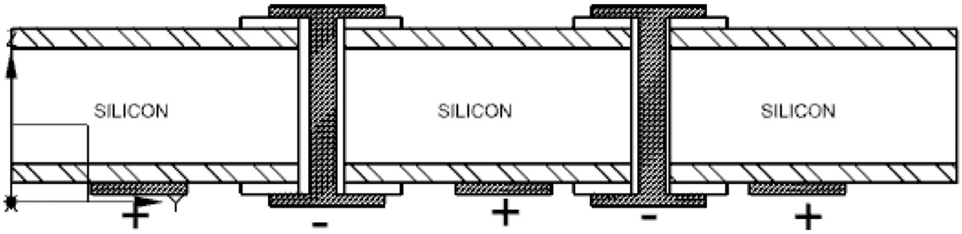


**Fig. 12.** Schematic of Pin-UP module cell interconnection.

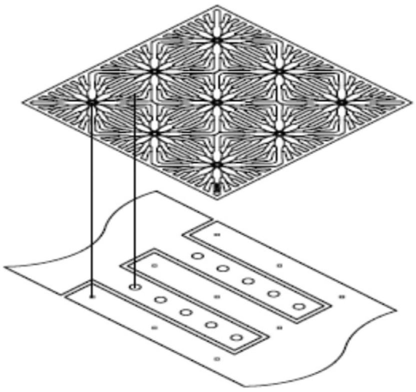

**Fig. 13.** Interconnection for a PUM one cell laminate.

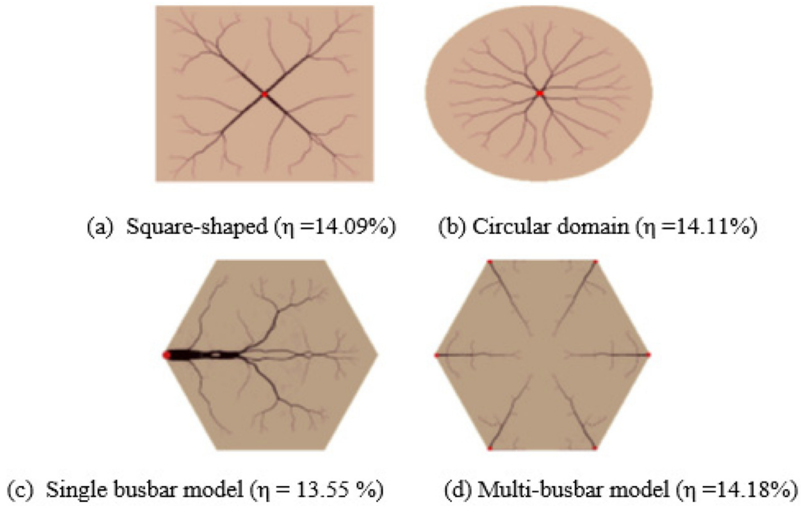


**Fig. 14.** Current innovations in PUM development [138].

plastic. Thermal arc spraying has the potential of forming a good connection but the mechanical strength generated by this interconnection method is not fully qualified. In principle, a thin foil can be used. However, since metal foil of such thickness is not readily available, a 50 $\mu$m thick foil is usually used [18] (Fig. 13).

The regular method for interconnection of PUM Cells involves the use of standard localised soldering technique to solder the pins to the front side of the silicon wafer. This is due to the relatively small soldering area available at the front of the cell. This soldering technique ensures that thermal stresses on the cells are minimised. Induced damage from the manufacture of the soldered joint from localised soldering is minimised. Also, this interconnection is not expected to be highly stressed at elevated temperatures as compared with the standard H-patterned interconnection. Some innovations in PUM development are shown in Fig 14.

The busbar (denoted by red) is located at the centroid of the geometry. The busbar extends from the centroid through the cell to the rear of the cell where all the interconnections are made. Generall, the circular-shaped PUM are expected to yield slightly high efficiencies compared with square-shaped PUMs. This is because for circular cells, the distance of the farthest

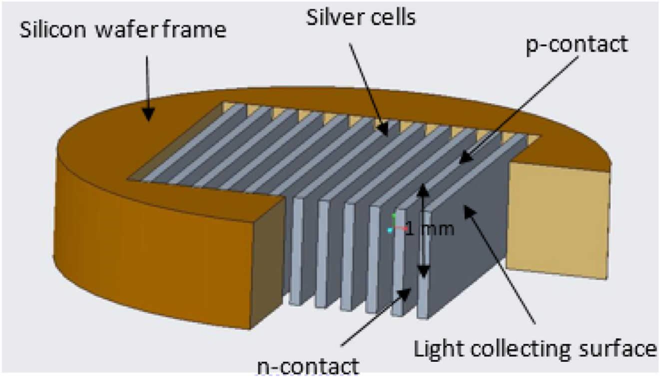


**Fig. 15.** Schematic drawing of Silver cells.

point from the busbar is shorter and that leads to relatively lower resistive losses [138]. Efficiency range of (13-14%) has so far been achieved for the new PUM interconnects. The innovative designs below were achieved by Topology Optimization.

*Silver solar cells*

Silver cells are made up of very thin monocrystalline silicon solar cell. The manufacturing technology involved in the production of silver cells allows for economic usage of silicon processed per module; with a reported 90–95% reduction by Franklin et al. [43]. The main step in forming the silvers is by micro machining deep and narrow grooves through the thick silicon wafers. The completed cells are subsequently removed and rotated through 90° for the larger area to form the sun-facing surface of the cell [137]. The metal contacts used for interconnection are located on the side of the silver - occupying a small fraction of the total surface of the cells. This arrangement eliminates shading due to metallization. Furthermore, doping below the contact could be made heavy resulting in excellent, low resistivity contacts with minimized recombination losses [34]. Fig 15 presents the schematic of solar silver cells.

Silver cells by design are very thin (around 50 $\mu$m) with emitter diffusions on both the front and rear surfaces. This arrangement offers a very high internal quantum efficiencies. High open-circuit voltages are possible with only relatively small minority carrier diffusion lengths in the bulk of the cell. This is an added advantage since the distance between sliver cell terminals is large enough (circa 1000 $\mu$m) for majority carrier drift in the bulk region. Such drift contribute significantly to series resistance losses unless low resistivity substrates (which have reduced diffusion length) are used [43]. Distributed series resistance losses present a major loss mechanism for the silver cell interconnect. Wider cells or cell operating under concentrated illumination are particularly affected. A closely related loss mechanism is attributed to a region of heavily compensated silicon which arises due to the overlap of the phosphorus sidewall emitter diffusion with sliver cell edge boron diffusion. The resulting loss is manifested in a reduced fill-factor and open-circuit voltage, corresponding to a distinct non-ideal recombination component. Current research is aimed at innovating a simplified cost effective manufacturing process capable of delivering cell efficiencies beyond 20% with superior energy yield.

*Spherical silicon solar cell interconnection*

The spherical (Sphelar) cell has a wrapped-up single-crystalline *p-n* junction reception surface that has enabled three-dimensional light capture and large reduction of silicon usage per meter$^2$ of module. The Sphelar solar cell employs a special manufacturing process technology which takes place under space-like conditions of microgravity. The process involves dripping molten silicon into a drop tube. As the molten silicon drops in a free-fall, it moulds into spheres due to the surface tension of the droplets. This process results in economic usage of silicon and the energy used in silicon cell production as compared with conventional technologies. According to *Taira et al* [127], the basic concept of Spherical cells is that a spherical sunlight reception surface can capture sunlight 3-dimensionally. This operation improves the power generation capacity to a maximum potential. Sphelar cells have comparatively higher efficiency than conventional cells having only one planar surface to capitalize upon sunlight. The schematic of spherical cell technology is presented in Fig 16.

The cell interconnection - consisting of small silver and aluminium electrodes on top and bottom of the spheres - is formed to produce a link between the emitter and base. The electrode arrangement enables an even distribution of generated current. Serial and or parallel cell interconnections can easily be facilitated [127]. If one outfitted the underside of the cell with a reflective material, the yield could be significantly enhanced [12]. The resulting interconnect geometry created by low temperature ECAs exhibits less induced stresses in the interconnect material. At elevated ambient temperature operation, the interconnection is likely to experience relatively lower thermal stresses. A Novel mono dispersed spherical $TiO_2$ aggregate with a diameter of 100 nm (SP100), which is the smallest $TiO_2$ spheres (or beads) reported thus far, has been prepared by a controlled hydrolysis and hydro thermal reaction. SP100 exhibits photovoltaic conversion efficiency of 18.41% with JSC of 22.91 mA/cm$^2$, VOC of 1049 mV and FF of 0.759 [144] (Fig. 17).

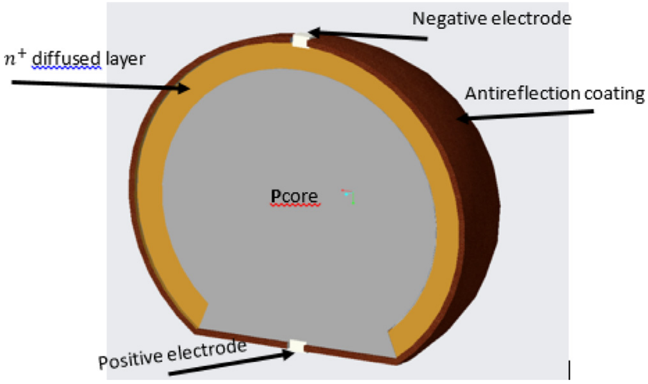


**Fig. 16.** Schematic of Spherical cell.

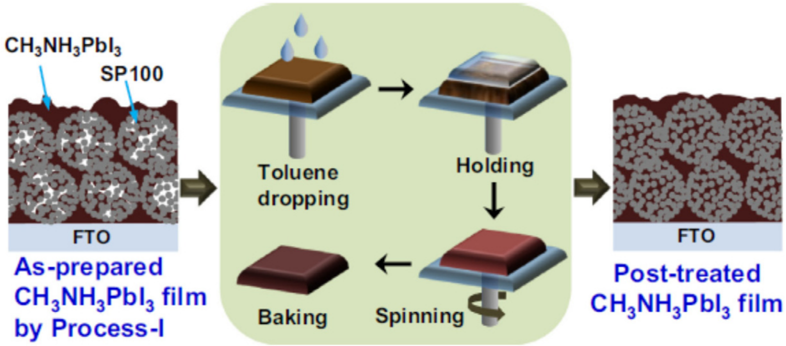


**Fig. 17.** SP100 Fabrication Process [144].

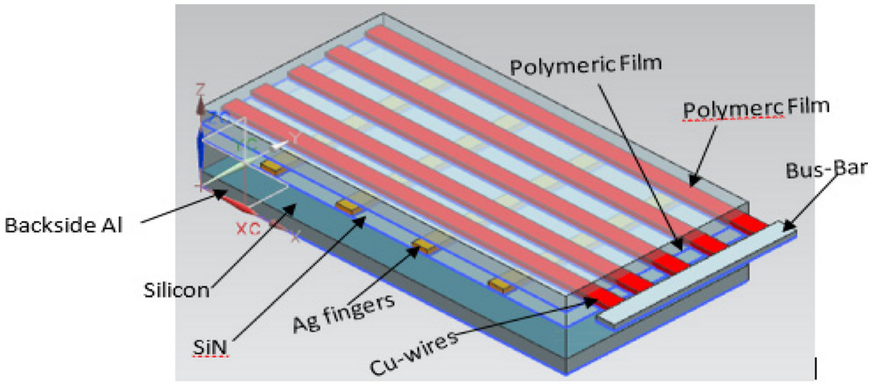


**Fig. 18.** Schematic of Day 4 Electrode.

*Solar cells with flexible electrode wire grid (Day4 Electrode)*

The solar cells with flexible electrode wire grid are also known as Day4TM Electrode. The solar cell technology is realized from a transparent compound of an adhesive and polymeric film with an embedded copper wire grid. The adhesive provides a dual functionality. It provides support as a housing for wires during the production of the electrode while providing the adhesion fixation on the solar cell through a standard lamination step with very low breaking yield [114]. The technology is shown in Fig 18.

The flexible nature of the electrode wire ensures a reliable cell interconnection. The design configuration ensures a stable fill-factor with almost no losses with reference to cell-level fill factor. The reduction of metallization area on the front and larger BSF passivation at the rear side of the Day4 solar cells increases Voc strongly. Though there appear to be a slightly higher shading from cells in 1-side lay-up using a 4-mm gap, it is compensated by an increase in encapsulation current. Rubin and Schneider [114] reported 0.1% increase in efficiency for Day4 cells in 1-side lay-up when compared with standard reference cells. They also reported 50% reduction in the amount of wires used for a 2-side lay-up which resulted in a reduction of cell shading (down to less than 6%) and with fill factor still at a higher level compared with standard cells. Day4 solar cells contacting architecture provides more than 2000 contacting points on the front side of the solar cell when compared with only two busing lines from standard solar cells. This unique contacting scheme secures a high interconnection redundancy against cell breakage. Experimental results from Rubin and Schneider [114] show only a small or no loss in cell power from cell breakage. At elevated temperatures, the induced thermal stresses are taken up by the narrow- sectioned wires, resulting in a nearly negligible thermal expansion and therefore a stable interconnection.

**R&D challenges and interconnection technologies evaluation of c-Si PV module for tropical climate suitability**

In this section, the factors affecting cell interconnection technologies such as cell interconnect technique, interconnect peel and residual strengths, average fill factor (FF), shading losses and power conversion efficiency (PCE) are reviewed. Furthermore, these factors are evaluated for their suitability for application in a tropical ambient.

The cell interconnect techniques

The standard soldering process, often by means of infrared heating, causes the complete tab-cell-tab package to be heated to a required soldering temperature for interconnection to be established. However, upon cooling, induced shear stress levels increase within the solder joint.

Subsequently, micro-cracks develop at the interface between the silicon cell and the silver-solder alloy. Propagation of the micro-cracks lead to lift-off and untimely failure of the interconnection. In addition to the standard soldering process, five different cell interconnection techniques are used for the realization of the various cell interconnection technologies. These techniques include: Infrared reflow (IR) soldering, laser spot soldering, electrically conductive adhesive (ECA), thermal arc spraying and ultrasonic welding.

In IR reflow soldering, a solder paste (a sticky mixture of powdered solder and flux) is used to temporarily attach the cell interconnectors. The entire assembly is subsequently subjected to controlled heat which melts the solder [142]. The IR reflow soldering allows minimum time above the liquidous solder temperature to reduce solder grain growth resulting in a more durable solder joint [10].

A laser spot soldering process where the power of the laser beam is controlled accurately to the desired spot lowers the temperature at which the joint is formed. The absorbed energy then heats the solder to its melting temperature, leading to soldering of the contact upon cooling. This completely eliminates any mechanical contact [110]. This soldering technique is desirable to minimize induces stress level [33]. Laser soldering usually uses a liquid state solder to wet the materials to be joined and provide mechanically and electrically stable connection when solidified [99]. Laser spot soldering, previously described in Section 2.3 Fig 6, delivers single solder spots amounting to 7-8 per busbar. The spot is evenly distributed over the busbar [143]. Such distribution impacts minimum mechanical damage on the soldered joint.

Electrically conductive Adhesives (ECA) are metal filled silicon-based adhesives that help create a reliable interconnection of solar cells–yielding high conductivity and flexibility while potentially reducing material costs ([27]. Accessed: 2017 January 14). Generally, a good conductive adhesive is not only determined by the electrical and mechanical properties after curing, but also depends on the curing characteristics [32,85]. The mechanical strength of the conductive adhesives is usually specified in terms of its shear strength and it is a function of size and materials of the test vehicles [32]. ECA offers increased flexibility and durability that improve the overall stability of PV module under thermal stress.

Thermal arc spraying involves heating metal powder with a thermal arc and spraying on the surfaces to be joined. This process leads to the realization of a very durable mechanical adhesion on the metal contacts whilst ensuring that cell and interconnecting material are kept at a lower temperature [17]. Ultrasonic welding employs a combination of friction and cold pressure welding applied at overlapped surfaces of interconnects to be welded together [47]. The process assumes an existing contact pressure during the welding. Contact forces and ultrasonic energy are applied simultaneously in such a manner that the required forces and the developing deformation of the parts being welded are greatly reduced. The key benefit of this interconnect technique is a reduction in induced mechanical stress build-up in the joint. Fig 19 presents the ranking of various interconnect technique in terms of induced mechanical stress magnitude.

From Fig. 19, IR soldering induces the highest stress in the interconnection. This is followed closely by spot soldering and ultrasonic welding. Mechanical clamping on the other hand, results in the lowest induced stress of the joint but the durability of the joint so formed remains a concern.

Interconnect peel strength

Peel strength of solar cell interconnect is the average load per unit width of bond line required to separate bonded interconnect ribbons where the angle of separation is 180° ([4] January 10). Peel strength is defined as the average force per unit width of bonded interconnect materials. Peel strength is part of the solar cell testing standard DINEN50461 and offers a very simple and quicker approach to measure the strength of adhesion of interconnector ribbons to solar cell metallization [40]. Table 2 present the peel strengths of various cell interconnect techniques discussed in Section 4.1. It can be observed from Table 2 that IR reflow soldering delivers interconnect with the highest peel strength (2-16) N. However, as shown in Fig 19, IR soldering introduces the highest induced mechanical stress in the interconnection. Mechanical clamping with unknown

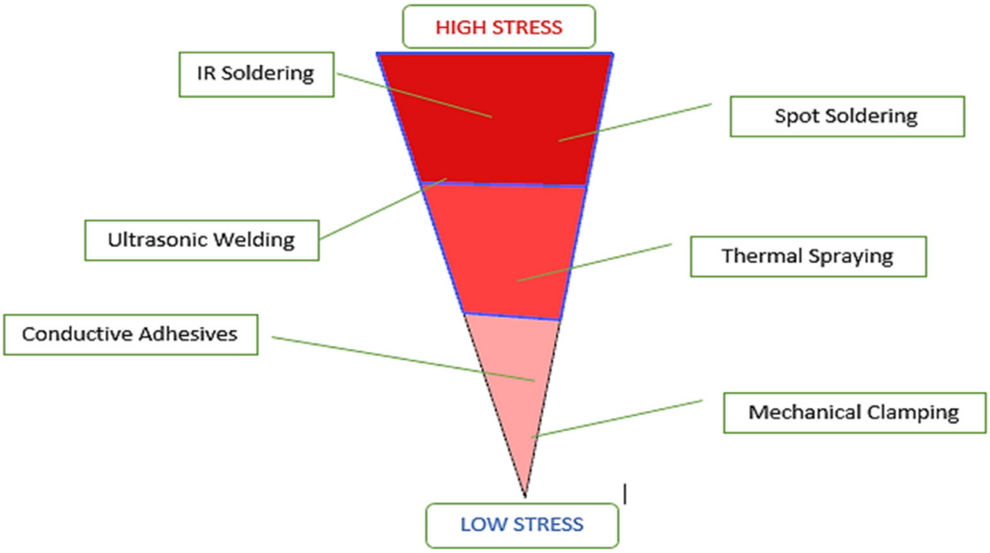


**Fig. 19.** Ranking of possible interconnection techniques in terms of induced mechanical stress.

**Table 1**
Comparison of interconnection techniques [104].

| Ribbon interconnection | Clamped | Soldered | Glued(ECA) |
|---|---|---|---|
| Long term stability | – | + | + |
| Mechanical stability | + | 0 | + |

peel strength delivers a relatively lower induced mechanical stress in the interconnection, which impacts favourably on the durability of the joint formed. At elevated PV module operating temperatures, characteristic of tropical climates, the joints formed are expected to be further subjected to induce thermo-mechanical stress.

The challenge therefore is to have an interconnect technique that can maintain the integrity of the joints formed under this harsh ambient condition. Table 1 summarizes the results of investigation from Pingel et al. [104]. The results show that soldering does induce stress to the cell which increases if thicker ribbons are used. In terms of long term reliability, soldering demonstrates better stability as interconnection technique than clamping. The use of ECA could be a compromise between higher power degradation compared to soldering but with less mechanical stress. A reduced ribbon thickness can also be adapted to reduce the stress introduced in cells during soldering. It will be a case of minimizing the overall costs keeping in mind the higher encapsulation losses for thinner ribbons.

Average Fill Factor (FF)

The fill factor (FF) is the ratio of the maximum power of the PV module to the virtual power (PT) that would result if Vmpp would be the open-circuit voltage and Impp would be the short-circuit current. FF is a performance indicator that measures the quality of the solar cell or PV module [76]. Although it cannot be practically achieved, an ideal PV module technology would produce a perfectly rectangular I-V curve in which the maximum power point coincided with (Isc, Voc) [120]. The FF can be interpreted graphically as the ratio of the area of the blue rectangle to the area of the green rectangle shown in Fig. 20.

Shading losses

Losses from shadow effect (optical losses) are caused by the presence of metal on the top surface of the solar cell which prevents light from penetrating the cell [6]. Shading losses are quantified as the fraction of the top surface of the cell covered by metal grid. It is determined by the transparency of the top surface which is caused by the width of the metal lines on the surface and the spacing of the metal lines [109]. Table 1 presents a tabular evaluation of the various interconnection technologies**.**

From Table 2, the IR soldering technique in conventional front-to-back, alternate p- and n-type, PUM and BJ-BC interconnections result in very high interconnect residual stress of (49-355) MPa. Furthermore, the thermal stress induced in these interconnections at elevated tropical ambient temperatures is likely to accelerate interconnect failure. The laser soldering on the other hand generates virtually no residual stresses on the EWT and MWT interconnections. Thus, induced thermal

**Table 2**
Comparison of cell interconnect technologies for c-Si solar cells in PV modules

| Cell interconnect technology | Interconnect technique | Interconnect peel strength (N) | Interconnect residual stress (MPa) | Average FF (%) | Shading losses (% of front cell area) | PCE (Maximum) (%) | | |
|---|---|---|---|---|---|---|---|---|
| | | | | | | Cell | Module | |
| | | | | | | | Lab. | Commercial |
| 1. Conventional Front-to-Back (H-patterned cell) | *IR soldering/ Laser spot soldering* (Ribbon-front-to-back) | (2-16) [81] (1-5) [121,122] | 49-355 [98] N/A | 71.8-75.4 [20,138] | 7 [129] | 18 [49] | | |
| 2. Emitter Wrapped Through (EWT) | *Laser soldering/ Electrical Conductive Adhesive (ECA)* (Edge Tab - back contact) | (1-5) [121,122] (0.3-1) [9] | N/A 15 - 19.5 [55] | 80 - 81 [68,82] | 3 | 21.6 [68] | | |
| 3. Metallization Wrap Through | *Laser soldering/ ECA* (conductive foil /ribbon*)* | (1-5) [121,122] (0.3-1) [9] | N/A 15 - 19.5 [55] | 76.6-78.4 [86,129] | 4.1[63] | 17.8 [83,143] | 17 [83] | |
| 4. BJ-BC | *IR soldering* (ribbon - back contact) | (2-16) [81] | 49- 355 [98] | 80.5 [125] | 0 [125] | 24 [49] | 22 [125] | 23.4 [125] |
| 5. Alternate p- and n-type cell | *IR soldering (*Ribbon-equivalent sides*)* | (2-16) [81] | 49- 355 [98] | 71.5 - 82.1 [13,16,78] | 1.6 - [113] | 21.8 [113] | | |
| 6. HoneyComb Design (HD) | *IR soldering/ ECA (Ribbon/Adhesive)* | (2-16) [81] (0.3-1) [9] | 49 -355 [98] 15 - 19.5 [55] | 68 [59] | 0 [59] | 19.8 [146] | 16.6 [59] | |
| 7. PUM cell | *IR soldering/ Thermal arc Spraying* (foils with patterned conductors) | (2-16) [81] N/A | 49-355 [98] N/A | 72-74.8 [20,138] | 6.5 [20] | 16.7 [91] | 13.8 [78] | 12.2 [78] |
| 8. Silver solar cells | *Solder bump* (substrate support bond) | (1–5) [121,122] | N/A | 81 [43] | 0 [43] | 20 [43] | 18.5 [43] | |
| 9. Spherical solar cells | *Ultrasonic welding (*substrate support bond) | (2 -5) [113] | N/A | 77.4-77.9 [12] | 0 [12] | 23.54 [12] | —— | —— |
| 10. Cell with flexible electrode wire | *ECA* (Day4 electrode wire) | (0.3-1) [9] | 15 - 19.5 [55] | 79 [114] | 6 [114] | 17 [114] | —— | —— |

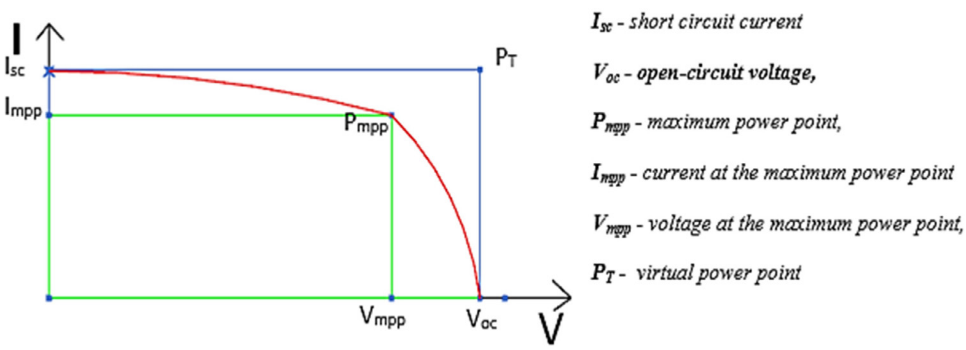


**Fig 20.** shows a schematic I-V curve of an illuminated PV module.

stresses resulting from elevated tropical ambient temperatures are unlikely to accelerate interconnect failure. In general, the interconnect peel strength resulting from IR soldering (2-16) *N* is relatively higher than that from laser soldering (1-5) N. However, the interconnect peel strength generated from the laser soldering is adequate to maintain the mechanical contact established by the joint during the soldering process.

A study of the average fill factors (FF) and shading losses of the interconnect technologies show that the BJ-BC interconnect offers the best combination of 80.5% (FF) and zero shading losses (0%). The EWT follow closely with a combination of (80-81% (FF)) and 3% shading losses. Finally, the power conversion efficiency (PCE) ratings for the various interconnection technologies reveal that the BJ-BC outputs the highest PCE of 24% at the cell level with the EWT following closely with a PCE of 21.6%.

## Effect of tropical climate on interconnection degradation factors on reliability of *c-Si PV module*

Tropical climates are characterised by average daily ambient temperature of 26 °C. The solar cell temperature rises to an average high of about 80 °C at mid-day and average low of about 15 °C at mid-night. Tropical climates also experiences high rainfall with occasional high winds and thunderstorms. An average relative humidity of about 85% is usually recorded. The above conditions incraeses the rate of degradation of interconnects of installed solar PV modules operating in the region. This section presents and discusses four factors accelerating the degradation of solder joints in crystalline silicon (c-Si) PV modules operating in tropical climates. The section presents the review in four sub-headings.

### Corrosion of solder joints and electrical contacts by diffusion of water vapour ingress into the encapsulant

Corrosion may be defined as a process of deterioration of materials due to chemical, physical or electrochemical reactions with the environment. The corrosion of metals typically proceeds as an electrochemical reaction since electrons may migrate in the metal and ions can be released to the environment [102]. The tropical climates are best described as *hot* and *humid*. The weather situation facilitates moisture intrusion into cells within the PV-module. When moisture permeates through the PV-module back-sheet or through edges of module laminates, it leads to cell corrosion that results to increase in leakage currents. EVA has relatively high diffusivity compared to most polymers and this makes it easier for moisture to enter the PV modules.

According to Kempe et al. [6], variation of diffusivities of polymers are by orders of magnitude. Significant reductions in water intrusion of cells is therefore feasible from different encapsulant materials Keeping a module completely dry for the PV module warranty period of 25 years may require low diffusivity materials such as Aclar (Polychlorotrifluoroethylene). However, most low diffusivity materials (including Aclar) have chllenges associated with adhesion. The use of such encapsulants could result in unacceptable delamination under enviromental exposure which would allow water to difuse into the module easier. Presence of water in PV module enhances corrosion process [101]. Corrosion significantly impacts negatively on the resistance properties of solder joints, cell metallization, cell interconnect bus-bars and junction-box terminations [101,139]. In turn, the effect reduces power produced by cells - leading to a drop in performance of the PV module. One other key functions of the encapsulant is to provide mechanical support to protect cells against breakage causes by impact during manufacture. Unfortunetly, materials with high mechanical strength such as PET and Aclar generally have low glass transition temperature ($T_g$) [29]. The property makes Aclar and PET unsuitable for use as encapsulant materials [30]. Materials with low $T_g$ have porous atomic structures and exhibits significant mobility. The porous structure tends to produce high diffusivities. Thus, the presence of low-modulus and low-$T_g$ is in conflict with low diffusivity. This situation severely limits potential benefits from materials that have low diffusivities which are potential substitutes for EVA. Even with impermeable front and back-sheets, moisture is still able to penerate the system and reach the centre of PV module in about two years due to the high diffusivity of EVA [66]. There is a growing interest in research focusing on water vapour limiting encapsulants capable of outperforming EVA in this regards. This is mainly due to the relatively high susceptibility of thin-film PV modules to water vapour [69]. Kim and Han [69] identify *ionome*r and *PVB* as potential candidates offering higher protection from environmental exposure for thin-film than EVA. Edge seal materials with low-diffusivity and dessicant are being investigated by several manufacturers [65]. These materials are capable of preventing moisture ingress over the lifetime of a module. Polyisobutylene (PIB) uniquely provides a very low moisture- permeability and diffusivity, as well as a low glass transition temperature [14,87]. Other edge seal materials (e.g. epoxies) can have very low diffusivities but they are hard and brittle and could easily crack or delaminate in a large module [65].

Though moisture is able to reach the centre of a module with impermeable front and back-sheets, it does not account for moisture-induced performance loss. However, moisture can saturate the outer few centimeters in a few months, enhancing corrosive process that can short out entire cells [50]. Super saturation of water around the edges of modules also accelerates delamination. The oxidative degradation of EVA may decrease the diffusivity of water, but it will increase the solubility of water by introduction of more polar groups leading to greater amount of water ingress [119]. Alternative encapsulants with superior adhesional strength and lower diffusivities could offer a better protection against hydrolytic reactions in the module. Although it has been experimentally demonstrated by Kempe et al. [65] that even a typical PV module will still approach equilibrium with the outside environment over 20 to 30-year lifetime of the module, the volume of water necessary to accelerate corrosion processes varies with the PV technology.

### Induced thermo-mechanical stress on solder joints occasioned by ambient temperature cycling

Tropical climatic conditions induce thermo-mechanical stresses in PV-modules due to ambient temperature cycling. Abrupt weather change represent a major long term reliability concerns in the PV-industry. Stresses are easily transferred from one cell to the adjacent interconnected cell as well as to the interconnectors. Locally induced stresses partly results from module temperature change. The induced stresses are caused majorly by the mismatch in the magnitude of the coefficients of thermal expansion (CTE) of the different materilas which include glass, interconnection, silicon wafer and Ag fingers that are bonded together in a PV module.

According to Gonzalez et al. [48], the higher CTE of glass relative to the cells makes the cells separate from each other occasioned by increase in temperature during the day. This causes a tensile stress in the interconnection. Gonzalez et al. [48] further observed that cells are pushed to each other upon cooling at night to temperatures lower than the stress free temperature condition, which causes compressive stress in the interconnection. The compressive stresses could lead to mechanical instability in the interconnection due to its thickness (-10 µm). PV module design is trending towards larger cells with shorter cell-to-cell interconnections. The challenge with this new designs is that large cells tend to exhibit significant relative displacements between cells. Owing to the shorter gap between cells, the capacity of modules to accommodate the deformation is jeopardised. The thermal cycling load for natural weathering caused by the alternation between day and night in the tropical climatic region is expected to be much lower compared with the IEC test conditions for thermal cycling at 125 K. The maximum temperature gradients observed for roof mounting in the region lie in the neighbourhood of 60 K. The highest yearly average of 37 K has also been reported. In this regard, the 125 K temperature gradient stipulated by IEC 61215 entails a much higher load on the materials due to thermomechanical stress. However, the larger number of cycles in long-term operation (approximately 9000 cycles for 25 years) at relatively lower temperature gradients may yield different material fatigue characteristics.

### Intermetallic compound Compound (IMC) growth in solder interconnects in PV module caused by ambient temperature thermal soaking and aging

Two types of IMC: $Cu_6Sn_5$ ($\eta$) and $Cu_3Sn$ ($\varepsilon$) are generally formed from the reaction between Sn and Cu in solar PV interconnection soldering [25,90,106]. A number of researchers including [35,134] explain that the $Cu_6Sn_5$ phase is typically formed above the melting point of the solder, while $Cu_3Sn$ phase is generally produced during low-temperature thermal aging (100 °C to 175 °C) by diffusion between Cu and $Cu_6Sn_5$.

The size (thickness) of an IMC layer greatly affects the reliability of the soldered joint. Pratt et al. [107] and Protsenko et al. [108] observed in their studies that a thin layer of IMC between the solder and Cu substrate improves bonding between solder and substrate but thicker IMC may have adverse impact on the toughness of the solder joints and interconnections. Several researchers have investigated the impact of IMC on the shear behaviour of solder/Cu joints. According to Alam and Co-authors [3,22,93,100], increasing thermal aging time or aging temperature leads to an increase in the thickness of the IMC layer. Deng et al. [36] further explains that the growth of intermetallic phases in the joint, both during soldering and lifetime, affects the quality of the joint and its reliability in terms of the mechanical response to applied loads. From research, isothermal aging severely affects several important material properties of solders such as; stiffness (modulus), yield stress, ultimate strength, and strain to failure. In their study, Ma et al. [88] observed a sharp change in the creep response of lead free solders, recording a 100 times increase in the steady state (secondary) creep strain rate (creep compliance) of Sn-Ag-Cu solders that were simply aged at room temperature.

In tropical climates, ambient temperatures are persistently above room temperature with an average daily high of 45 °C and an average of eight hours of continuous sunshine. Thus, the thermal soaking and aging of solder interconnects in PV modules is likely to occur through continuous exposure of modules over long periods of elevated tropical temperature.

The mechanical properties of the IMC layer at the solder interconnections in the module deteriorates. The change is expected to adversely affect the strength of the solder interconnections.

Presence of micro-cracks in PV module caused by vibrations resulting from hail storms and high winds

Micro cracks can develop in cell of PV module during manufacturing, transportation or exposure in service. Repeated climatic events such as snow loads, hailstorms or strong winds increases the crack size and cause its propagation [5,73,77,103]. Tropical climates are characterized by occasional hailstorms and high winds which can trigger cracks in the front glass and in the cell of the PV-module. Wind loads are highly dynamic and thus triggers oscillations. Dynamic loads are known to induce fatigue loads on the materials - especially on PV-cells and connecting wires [140]. When cracks develop in the interconnection circuit of cells, they may create potential locations for heating if both interconnects of a cell are affected by material fatigue. In the worst case, arcing may occur if the conditions for arc ignition are fulfilled [57,111]. Defects from micro-cracks coupled with poor electrical contacts tend to reduce the lifetime of the PV-module in the field [23].

The orientation of a crack could have varied impact on the power delivery of a PV module. According to Grunow et al. [51,75], a single crack which is oriented in a way that leads to an electrical separation of a relevant part of the cell could severely affect the power delivery of a PV module. In contrast, cracks that do not lead to an interconnection brake marginally affect the performance of a PV module. A detailed complementary study on crack formation after the mechanical load test also demonstrated that many cracks, about 50%, were found parallel to the busbars, thus causing maximum degradation in cell and overall module performance [64]. These cracks may lead to the disconnection of cell parts and thus power loss [96]. High winds causes dynamic loading on PV-cells and can create contact problems from bad soldering of cell interconnection. This could result in increased power losses from PV-modules. Investigations from Koch et al. [72] reveal that dynamic mechanical loading affects the mechanical robustness of solder contacts in PV-modules and could lead to a total interconnection failure.

## Summary

Interconnection technologies employed in the manufacture of crystalline silicon photovoltiac (c-Si PV) module are reviewed for application in the manufacture of robust module for increased thermo-mechnical reliability during operations in tropical climate. The factors accelerating degradation of solder joints in c-Si PV interconnection operating in tropical regions are also reviewed and discussed. The review identified back-contacted solar cells (BC) design as the architecture that potentially eliminates recombination losses. Similalry, the EWT cell architecture is found to record higher cell efficiencies up to 21.6% while the MWT cell design demonstrates initial superior energy yield compared with conventional solar cells. It is found that the alternate p- and n- type interconnections offers a simpler interconnection procedure and a higher yield during module fabrication while the Honeycomb design produces excellent packing density that reduces the ‘double bounce’ effect.

The review revealed that the amount of water necessary to accelerate corrosion process in PV modules is yet to be quantified. It identified that the temperature cycling load from natural weathering in the tropical ambient is lower than the load from IEC 61215 test conditions. However, the larger number of cycles produced by natural weathering test conditions within the region may culminate in different material fatigue yield characteristics. The research findings reveal that isothermal aging leads to about 50% reductions in several key material properties including stiffness, yield stress and ultimate strength.

It is identifiied that significant amount and intensity of hail storms and high winds that characterise the region make micro-cracks to develep in the cells and cause untimely module failure. The phonomenon excessively incresases the dynamic loads on the modules and negatively impacts on module mechanical integrity and reliability. The elevated ambient temperatures increases the rate of IMC growth in the interconnection of modules – leading the modules operating in the region to increasing interconnection failure.

More review results show that BJ-BC interconnect technology has the highest PCE of 23.4% at commercial level while spherical solar cells demonstrtaes potential of generating a relatively higher PCE of 23.54% at cell and laboratory level. The use of electrical conductive adhesives (ECA) for cell interconnection is found to produce module with relative lower residual stresses of 15-195 MPa. The challenge to the adoption of ECAs is that the usage results to low interconnect peel strength in the range of 0.3-1.0 MPa - which could further deteriorate during module operation in elevated tropical ambient temperature. It is found that infra-red reflow soldering induces high mechanical stress in the solder joints of the module which will have nagetive effect at elevated temperature operation. Selective laser soldering technique is found to be capable of reducing the impact of induced thermo-mechanical stress on PV cell interconnection. Considering the results of the review, the authors propose a BJ-BC interconnection technology with selective laser soldering technique as the architecture and technology poised to yield robust c-Si PV module for application in tropical ambient.

## Declaration of Competing Interest

We declare that there is no conflict of interest with this publication. Furthermore, financial support for this work did not influence the outcome.

## Acknowledgement

The authors acknowledge the financial support received from the USAID for the PRESSA project Sub-Grant no. 2000004829 through the US National Academy of Sciences. The technical support provided by Dr. Mani and Sai Tatapudi at Arizona State University Photovoltaic Reliability Laboratory (ASU PRL) is greatly appreciated.

## Reference

[1] A. Faes, M. D., J. Levrat, J. Champliaud, A. Lachowicz, J. Geissbühler, N. Badel, H. Watanabe, T. Söderström, Y. Y., J. Ufheil, P. Papet, B. Strahm, J. Hermans, A. Tomasi, Y. Baumgartner, J. Cattin, M., A.H.-W. Kiaee, J. Fleischer, P.V. Fleischer, A. Tsuno, C. BallifS, Advanced metallization enabled by smart-wire interconnection for silicone heterojunction cell, presentation at 6th workshop on metallization and interconnection for crystalline silicon solar cells, Energy Procedia 98 (2016) 2–11.

[2] A. Aberle, S. Wenham, M. Green, A new method for accurate measurements of the lumped series resistance of solar cells, Paper presented at the Photovoltaic Specialists Conference, 1993., Conference Record of the Twenty Third IEEE, 1993.

[3] M. Alam, Y. Chan, K. Hung, Reliability study of the electroless Ni–P layer against solder alloy, Microelectron. Reliab. 42 (7) (2002) 1065–1073.

[4] Ametektest. (Accessed: 2017 January 10). HYPERLINK " Http://www.Ametektest.Com/learningzone/testtypes/peel-strength-testing .

[5] M. Assmus, S. Jack, K.A. Weiss, M. Koehl, Measurement and simulation of vibrations of pv-modules induced by dynamic mechanical loads, Progr. Photovolt. 19 (6) (2011) 688–694.

[6] C. Baccouch, H. Sakli, D. Bouchouicha, T. Aguili, Patch antenna based on a photovoltaic solar cell grid collection, Paper presented at the Progress in Electromagnetic Research Symposium (PIERS), 2016.

[7] A. Balaska, A. Tahri, F. Tahri, A.B. Stambouli, Performance assessment of five different photovoltaic module technologies under outdoor conditions in algeria, Renew. Energy 107 (2017) 53–60.

[8] G. Beaucarne, Materials challenge for shingled cells interconnection, Energy Procedia 98 (2016) 115–124.

[9] I Bennett, B. Geerligs, C Olson, M. Goris, Compatibility of Copper-Electroplated Cells with Metal Wrap-Through Module Materials, 2013 http://www.sustainablepv.eu/fileadmin/sustainablepv/user/PVI21_Paper_08_ECN_Modules_v4.pdf.

[10] J. Bergenthal, Reflow Soldering Process Considerations for Surface Mount Application, 1995, pp. 2–3.

[11] V. Bheemreddy, B.J. Liu, Methodology for predicting flexible photovoltaic cell life using accelerated tests, Paper presented at the 2019 IEEE 46th Photovoltaic Specialists Conference (PVSC), 2019.

[12] M. Biancardo, K. Taira, N. Kogo, H. Kikuchi, N. Kumagai, N. Kuratani, …, J. Nakata, Characterization of microspherical semi-transparent solar cells and modules, Solar Energy 81 (6) (2007) 711–716, doi:10.1016/j.solener.2006.10.009.

[13] S. Bordihn, V. Mertens, J. Cieslak, G. Zimmermann, R. Lantzsch, J. Scharf, …, S. Laube, Status of industrial back junction n-type Si solar cell development, Energy Procedia 92 (2016) 678–683.

[14] R.H. Boyd, P.K. Pant, Molecular packing and diffusion in polyisobutylene, Macromolecules 24 (23) (1991) 6325–6331.

[15] S. Braun, G. Hahn, R. Nissler, C. Pönisch, D. Habermann, Multi-busbar solar cells and modules: high efficiencies and low silver consumption, Energy Procedia 38 (2013) 334–339.

[16] T. Buck, R. Kopecek, J. Libal, R. Petres, K. Peter, I. Rover, ..., P. Fath, *Large area screen printed n-type Mc-Si solar cells with b-emitter: efficiencies close to 15% and innovative module interconnection*, Paper presented at the Photovoltaic Energy Conversion, Conference Record of the 2006 IEEE 4th World Conference on, 2006.

[17] J. Bultman, D. Eikelboom, R. Kinderman, A. Tip, A. Weeber, M. Meuwissen, …, F. Schuurmans, Selecting optimal interconnection methodology for easy and cost efficient manufacturing of the pin up module, in: Paper presented at the Proceedings of the PV In Europe—From PV Technology to Energy Solutions, Rome, 2002.

[18] J. Bultman, A. Weeber, M. Brieko, J. Hoornstra, A. Burgers, J. Dijkstra, …, F. Schuurmans, Pin up module: a design for higher efficiency, easy module manufacturing and attractive appearance, in: Paper Presented at the Proceedings of the 16th EPVSC, Glasgow, 2000.

[19] J.H. Bultman, M.W. Brieko, A.R. Burgers, J. Hoornstra, A.C. Tip, A.W. Weeber, Interconnection through vias for improved efficiency and easy module manufacturing of crystalline silicon solar cells, Solar Energy Mater. Solar Cells 65 (1–4) (2001) 339–345, doi:10.1016/S0927-0248(00)00111-2.

[20] JH Bultman, W. A., MW Brieko, J Hoornstra, AR Burgers, Dijkstra, Pin up Module: A Design for Higher Efficiency, Easy Module Manufacturing and Attractive Appearance, 2012 Retrieved from http://www.ecn.nl/docs/library/report/2000/rx00010.pdf .

[21] C. Cañete, J. Carretero, M. Sidrach-de-Cardona, Energy performance of different photovoltaic module technologies under outdoor conditions, Energy 65 (2014) 295–302.

[22] Y. Chan, A.C. So, J. Lai, Growth kinetic studies of Cu–Sn intermetallic compound and its effect on shear strength of LCCC smt solder joints, Mater. Sci. Eng. B 55 (1) (1998) 5–13.

[23] P. Chaturvedi, B. Hoex, T.M. Walsh, Broken metal fingers in silicon wafer solar cells and pv modules, Solar Energy Mater. Solar Cells 108 (2013) 78–81, doi:10.1016/j.solmat.2012.09.013.

[24] X. Chen, K. Church, H. Yang, I.B. Cooper, A. Rohatgi, Improved front side metallization for silicon solar cells by direct printing, Paper presented at the Photovoltaic Specialists Conference (PVSC), 2011 37th IEEE, 2011.

[25] W.K. Choi, S.-Y. Jang, J.H. Kim, K.-W. Paik, H.M. Lee, Grain morphology of intermetallic compounds at solder joints, J. Mater. Res. 17 (03) (2002) 597–599.

[26] J.-P. Clech, Acceleration factors and thermal cycling test efficiency for lead-free Sn-Ag-Cu assemblies, in: Paper Presented at the Proceedings, SMTA International Conference, Chicago, IL, 2005.

[27] D.C. Corporation, Electrically Conductive Adhesives Accessed: 2017 January 14, 2013 *https://www.dowcorning.com/content/solar/solarproducts/Electrically_Conductive_Adhesives.aspx*.

[28] G. Cuddalorepatta, A. Dasgupta, S. Sealing, J. Moyer, T. Tolliver, J. Loman, Durability of pb-free solder connection between copper interconect wire and crystalline silicon solar cells, Paper presented at the Thermal and Thermomechanical Phenomena in Electronics Systems, 2006. ITHERM '06. The Tenth Intersociety Conference on, 2006.

[29] E. Cuddihy, C. Coulbert, A. Gupta, R. Liang, Electricity from photovoltaic solar cells: flat-plate solar array project final report, Volume vii: Module Encapsulation, 1986.

[30] Cuddihy, E., Coulbert, C., Liang, R., Gupta, A., Willis, P., & Baum, B. (1983). Applications of ethylene vinyl acetate as an encapsulation material for terrestrial photovoltaic modules.

[31] K.O. Davis, M.P. Rodgers, G. Scardera, R.P. Brooker, H. Seigneur, N. Mohajeri, …, W.V. Schoenfeld, Manufacturing metrology for C-Si module reliability and durability Part II: cell manufacturing, Renew. Sustain. Energy Rev. 59 (2016) 225–252, doi:10.1016/j.rser.2015.12.217.

[32] P. De Jong, D. Eikelboom, R. Kinderman, A. Tip, J. Bultman, M. Meuwissen, M. Van den Nieuwenhof, Single-step laminated full-size pv modules made with back-contacted mc-Si cells and conductive adhesives, in: 19th EPVSEC, Paris, 2004, p. 2145.

[33] P.C. de Jong, D. Eikelboom, J. Wienke, M. Brieko, M. Kloos, Low-stress interconnections for solar cells, Paper presented at the Presented at the 20th European Photovoltaic Solar Energy Conference and Exhibition, 2005.

[34] P.N. Deenapanray, C. Athukorala, D. Macdonald, W. Jellett, E. Franklin, V. Everett, …, A. Blakers, Reactive ion etching of dielectrics and silicon for photovoltaic applications, Progr. Photovolt. 14 (7) (2006) 603–614.

[35] X. Deng, G. Piotrowski, J. Williams, N. Chawla, Influence of initial morphology and thickness of $Cu_6Sn_5$ and $Cu_3Sn$ intermetallics on growth and evolution during thermal aging of Sn-Ag solder/cu joints, J. Electron. Mater. 32 (12) (2003) 1403–1413.

[36] X. Deng, R. Sidhu, P. Johnson, N. Chawla, Influence of reflow and thermal aging on the shear strength and fracture behavior of Sn-3.5 Ag solder/Cu joints, Metall. Mater. Trans. A 36 (1) (2005) 55–64.
[37] N.G. Dhere, N.R. Raravikar, Adhesional shear strength and surface analysis of a pv module deployed in harsh coastal climate, Solar Energy Mater. Solar Cells 67 (1–4) (2001) 363–367, doi:10.1016/S0927-0248(00)00304-4.
[38] A.S.A. Diniz, D.A. Cassini, M.C. de Oliveira, V.F. de Lins, M.M. Viana, D.S. Braga, L.L. Kazmerski, Evaluation of performance losses and degradation of aged crystalline si photovoltaic modules installed in Minas Gerais (Brazil), Renew. Energy Sustain. Build. (2020) 29–46.
[39] D. Eikelboom, J. Bultman, A. Schönecker, M. Meuwissen, M. Van Den Nieuwenhof, D. Meier, Conductive adhesives for low-stress interconnection of thin back-contact solar cells, Paper presented at the Photovoltaic Specialists Conference, 2002. Conference Record of the Twenty-Ninth IEEE, 2002.
[40] U. Eitner, L. Rendler, Peel testing of ribbons on solar cells at different angles: consistent comparison by using adhesive fracture energies, in: Proc. of the 29th EUPVSEC, Amsterdam, 2014, pp. 3406–3408.
[41] E. Elibol, Ö.T. Özmen, N. Tutkun, O. Köysal, Outdoor performance analysis of different pv panel types, Renew. Energy Sustain. Build. 67 (2017) 651–661, doi:10.1016/j.rser.2016.09.051.
[42] A. Faes, M. Despeisse, J. Levrat, J. Champliaud, N. Badel, M. Kiaee, …, M. Gragert, Smartwire solar cell interconnection technology, in: Paper presented at the Proc. 29th Eur. Photovoltaic Sol. Energy Conf, 2014.
[43] E. Franklin, A. Blakers, K. Weber, V. Everett, P. Deenapanray, Towards a simplified 20% efficient sliver cell, Paper presented at the Photovoltaic Energy Conversion, Conference Record of the 2006 IEEE 4th World Conference on, 2006.
[44] A.M. Gabor, M. Ralli, S. Montminy, L. Alegria, C. Bordonaro, J. Woods, …, T. Williams, Soldering induced damage to thin si solar cells and detection of cracked cells in modules, Paper presented at the 21st European Photovoltaic Solar Energy Conference, 2006 September.
[45] W. Gambogi, B.-L. Yu, T. Felder, S. MacMaster, K.R. Choudhury, J. Tracy, …, H. Hu, Development of accelerated test sequences to assess long term durability of pv modules, Paper presented at the 2019 IEEE 46th Photovoltaic Specialists Conference (PVSC), 2019.
[46] J.M. Gee, W.K. Schubert, P.A. Basore, Emitter wrap-through solar cell, Paper presented at the Photovoltaic Specialists Conference, 1993., Conference Record of the Twenty Third IEEE, 1993.
[47] Gochermann, H. (1990). Apparatus for Welding Components Together with the use of ultr$asound. In: Google Patents.
[48] M. Gonzalez, J. Govaerts, R. Labie, I. De Wolf, K. Baert, Thermo-mechanical challenges of advanced solar cell modules, Paper presented at the Thermal, Mechanical and Multi-Physics Simulation and Experiments in Microelectronics and Microsystems (EuroSimE), 2011 12th International Conference on, 2011.
[49] F. Granek, C. Reichel, Back-contact back-junction silicon solar cells under UV illumination, Solar Energy Mater. Solar Cells 94 (10) (2010) 1734–1740.
[50] N. Grossiord, J.M. Kroon, R. Andriessen, P.W. Blom, Degradation mechanisms in organic photovoltaic devices, Organ. Electron. 13 (3) (2012) 432–456.
[51] P. Grunow, P. Clemens, V. Hoffmann, B. Litzenburger, L. Podlowski, Influence of micro cracks in multi-crystalline silicon solar cells on the reliability of pv modules, in: Proceedings of the 20th EUPVSEC, 2005, pp. 2042–2047.
[52] J.-H. Guo, J.E. Cotter, Laser-grooved backside contact solar cells with 680-mv open-circuit voltage, IEEE Trans. Electron Devices 51 (12) (2004) 2186–2192.
[53] R. Hall, T. Soltys, Polka dot solar cell, Paper presented at the 14th Photovoltaic Specialists Conference, 1980.
[54] X. Han, Y. Wang, L. Zhu, H. Xiang, H. Zhang, Mechanism study of the electrical performance change of silicon concentrator solar cells immersed in de-ionized water, Energy Convers. Manag. 53 (1) (2012) 1–10, doi:10.1016/j.enconman.2011.08.011.
[55] M.K. Hasan, K. Sasaki, Thermal deformation analysis of tabbed solar cells using solder alloy and conductive film, J. Mech. Sci. Technol. 30 (7) (2016) 3085–3095.
[56] M. Hendrichs, B. Thaidigsmann, T. Fellmeth, S. Nold, A. Spribille, P. Herrmann, …, F. Clement, Cost-optimized metallization layout for metal wrap through (MWT) solar cells and modules, in: Paper Presented at the Proceedings of the 28th European Photovoltaic Solar Energy Conference and Exhibition, Paris, 2013.
[57] Herrmann, W., Bogdanski, N., Reil, F., Köhl, M., Weiss, K. A., Assmus, M., & Heck, M. (2010). *Pv module degradation caused by thermomechanical stress: real impacts of outdoor weathering versus accelerated testing in the laboratory*.
[58] R. Hoenig, F. Clement, M. Menkoe, M. Retzlaff, D. Biro, R. Preu, …, W. Zhang, Paste development for screen printed mc-Si mwt solar cells exceeding 17% efficiency, Paper presented at the Photovoltaic Specialists Conference (PVSC), 2010 35th IEEE, 2010.
[59] C.K. Huang, K.W. Sun, W.L. Chang, Efficiency enhancement of silicon solar cells using a nano-scale honeycomb broadband anti-reflection structure, Opt. Express 20 (S1) (2012) A85–A93, doi:10.1364/OE.20.000A85.
[60] R. Hulstrom, Pv *Module Reliab*ility *R* & *D Project Overvie*w, 2005.
[61] IEC61215, Crystalline silicon terrestrial pvmodules, Design Qualification and Type Approval, 61215, IEC, Geneva, Switzerland, 1993.
[62] J.-S. Jeong, N. Park, C. Han, Field failure mechanism study of solder interconnection for crystalline silicon photovoltaic module, Microelectron. Reliab. 52 (9–10) (2012) 2326–2330, doi:10.1016/j.microrel.2012.06.027.
[63] C Jordan Dirk, K. S. R., Photovoltaic degradation rates—an analytical review, Progr. Photovolt. 21 (1) (2013) 12–29.
[64] S. Kajari-Schröder, I. Kunze, U. Eitner, M. Köntges, Spatial and orientational distribution of cracks in crystalline photovoltaic modules generated by mechanical load tests, Solar Energy Mater. Solar Cells 95 (11) (2011) 3054–3059, doi:10.1016/j.solmat.2011.06.032.
[65] M. Kempe, A. Dameron, T. Moricone, M. Reese, Evaluation and modeling of edge-seal materials for photovoltaic applications, Paper presented at the Photovoltaic Specialists Conference (PVSC), 2010 35th IEEE, 2010.
[66] M.D. Kempe, Modeling of rates of moisture ingress into photovoltaic modules, Solar Energy Mater. Solar Cells 90 (16) (2006) 2720–2738, doi:10.1016/j.solmat.2006.04.002.
[67] E.V. Kerschaver, G. Beaucarne, Back-contact solar cells: a review, Progr. Photovolt. 14 (2) (2006) 107–123, doi:10.1002/pip.657.
[68] F. Kiefer, C. Ulzhofer, T. Brendemuhl, N.P. Harder, R. Brendel, V. Mertens, …, J.W. Muller, High efficiency n-type emitter-wrap-through silicon solar cells, IEEE J. Photovolt. 1 (1) (2011) 49–53, doi:10.1109/JPHOTOV.2011.2164953.
[69] N. Kim, C. Han, Experimental characterization and simulation of water vapor diffusion through various encapsulants used in pv modules, Solar Energy Mater. Solar Cells 116 (2013) 68–75.
[70] D.L. King, B. W. E., J.A. Kratochvil, Photovoltaic Array Performance Model, 2004 Retrieved from Albuquerque, New Mexico.
[71] R. Klengel, M. Petzold, D. Schade, B. Sykes, Improved testing of soldered busbar interconnects on silicon solar cells, Paper Presented at the Microelectronics and Packaging Conference (EMPC), 2011 18th European, 2011.
[72] S. Koch, J. Kupke, D. Tornow, M. Schoppa, S. Krauter, P. Grunow, Dynamic mechanical load tests on crystalline silicon modules, Paper presented at the 25th European Photovoltaic Solar Energy Conference–Valencia, 2010.
[73] C. Kohn, R. Kübler, M. Krappitz, G. Kleer, I. Reis, M. Retzlaff, …, D. Biro, Influence of the metallization process on the strength of silicon solar cells, Paper Presented at the 24th European Photovoltaic Solar Energy Conference, 2009.
[74] M. Köntges, V. Jung, U. Eitner, Requirements on metallization schemes on solar cells with focus on photovoltaic modules, Paper Presented at the 2nd Workshop on Metallization of Crystalline Silicon Solar Cells, 2010.
[75] M. Köntges, I. Kunze, S. Kajari-Schröder, X. Breitenmoser, B. Bjørneklett, The risk of power loss in crystalline silicon based photovoltaic modules due to micro-cracks, Solar Energy Mater. Solar Cells 95 (4) (2011) 1131–1137, doi:10.1016/j.solmat.2010.10.034.
[76] M. Kontges, S. Kurtz, C. Packard, U. Jahn, K. Berger, K. Kato, …, M. Van Iseghem, Performance and Reliability of Photovoltcaic Systems–Subtask 3.2: Review of Failures of Photovoltaic Modules, 2014 External final report by international energy agency (IEA) for photovoltaic power systems programme (PVPS).
[77] M. Köntges, M. Siebert, A. de la Dedicación Rodríguez, M. Denz, M. Wegner, R. Illing, F. Wegert, Impact of transportation on silicon wafer-based pv modules, in: Paper Presented at the Proc. 28th Eur. Photovoltaic Sol. Energy Conf, 2013.

[78] R. Kopecek, T. Buck, A. Kränzl, J. Libal, K. Peter, A. Schneider, …, E. Wefringhaus, Module interconnection with alternate p-and n-type si solar cells, in: Proc. 21th EUPVSC Dresden Germany, 2006.
[79] R. Kopecek, T. Buck, J. Libal, I. Rover, K. Wambach, L.J. Geerligs, …, P. Fath, Large area screen printed n-type silicon solar cells with rear aluminium emitter: efficiencies exceeding 16%, Paper presented at the Photovoltaic Energy Conversion, Conference Record of the 2006 IEEE 4th World Conference on, 2006.
[80] R. Kopecek, J. Libal, T. Buck, K. Peter, K. Wambach, M. Acciarri, …, P. Fath, N-type multicrystalline silicon: material for solar cell processes with high efficiency potential, in: Paper presented at the Conference Record of the Thirty-first IEEE Photovoltaic Specialists Conference, 2005, p. 2005.
[81] F. Kraemer, S. Wiese, E. Peter, J. Seib, Mechanical problems of novel back contact solar modules, Microelectron. Reliab. 53 (8) (2013) 1095–1100, doi:10.1016/j.microrel.2013.02.019.
[82] D. Kray, J. Dicker, S. Rein, F. Kamerewerd, D. Osswald, E. Schäffer, …, G. Willeke, High-efficiency emitterwrap-through cells, in: Proceedings of the 17th EPVSC, Munich, 2001, pp. 1299–1302.
[83] M. Lamers, C. Tjengdrawira, M. Koppes, I. Bennett, E. Bende, T. Visser, …, I. Romijn, 17.9% metal-wrap-through mc-si cells resulting in module efficiency of 17.0%, Progr. Photovolt. 20 (1) (2012) 62–73.
[84] O. Leistiko, The waffle: a new photovoltaic diode geometry having high efficiency and backside contacts, Paper presented at the Photovoltaic Energy Conversion, 1994., Conference Record of the Twenty Fourth. IEEE Photovoltaic Specialists Conference-1994, 1994 IEEE First World Conference on, 1994.
[85] J. Liu, Z. Lai, H. Kristiansen, C. Khoo, Overview of conductive adhesive joining technology in electronics packaging applications, in: Paper presented at the Adhesive Joining and Coating Technology in Electronics Manufacturing, 1998. Proceedings of 3rd international Conference on, 1998.
[86] E. Lohmuller, B. Thaidigsmann, M. Pospischil, U. Jager, S. Mack, J. Specht, …, F. Clement, 20% efficient passivated large-area metal wrap through solar cells on boron-doped cz silicon, IEEE Electron Device Lett. 32 (12) (2011) 1719–1721.
[87] J. Lundberg, E. Mooney, C. Rogers, Diffusion and solubility of methane in polyisobutylene, J. Polym. Sci. Part A-2 7 (5) (1969) 947–962.
[88] H. Ma, J.C. Suhling, P. Lall, M.J. Bozack, Reliability of the aging lead free solder joint, Paper Presented at the 56th Electronic Components and Technology Conference 2006, 2006.
[89] M. Macben, T. Nelson, B. Mutua, A. Ismael, Degradation prevalence study of field-aged photovoltaic modules operating under Kenyan climatic conditions, Sci. J. Energy Eng. 3 (2015) 1–5.
[90] Z. Mei, A. Sunwoo, J. Morris, Analysis of low-temperature intermetallic growth in copper-tin diffusion couples, Metall. Trans. A 23 (3) (1992) 857–864.
[91] R. Meier, F. Kraemer, S. Wiese, K.-J. Wolter, J. Bagdahn, Reliability of copper-ribbons in photovoltaic modules under thermo-mechanical loading, Paper Presented at the Photovoltaic Specialists Conference (PVSC), 2010 35th IEEE, 2010.
[92] Y. Meydbray, K. Wilson, E. Brambila, A. Terao, S. Daroczi, Solder joint degradation in high efficiency all back contact solar cells, in: Paper Presented at the Proceedings of the 22th European Photovoltaic Solar Energy Conference, Milan, Italy, 2007 September.
[93] H.-W. Miao, J.-G. Duh, Microstructure evolution in Sn–Bi and Sn–Bi–Cu solder joints under thermal aging, Mater. Chem. Phys. 71 (3) (2001) 255–271.
[94] H.J. Möller, Wafer processing, in: Handbook of Photovoltaic Silicon, 2019, pp. 269–309.
[95] K. Morita, T. Inoue, H. Kato, I. Tsuda, Y. Hishikawa, Degradation factor analysis of crystalline-si pv modules through long-term field exposure test, in: Paper Presented at the Photovoltaic Energy Conversion, 2003. Proceedings of 3rd World Conference on, 2003.
[96] A. Morlier, F. Haase, K. M, Impact of cracks in multicrystalline silicon solar cells on pv module power ;a simulation study based on field data, IEEE J. Photovolt. 5 (6) (2015) 1735–1741, doi:10.1109/JPHOTOV.2015.2471076.
[97] D.-H. Neuhaus, A. Münzer, Industrial silicon wafer solar cells, Adv. OptoElectron. 2007 (2008).
[98] M. Novotny, L. Jakubka, P. Cejtchaml, I. Szendiuch, Thermomechanical stressing of solar cells, Paper presented at the Thermal, Mechanical and Multiphysics Simulation and Experiments in Micro-Electronics and Micro-Systems, 2006. EuroSime 2006. 7th International Conference on, 2006.
[99] E.S. Ogochukwu, Laser Soldering, 2013.
[100] H. Pang, K. Tan, X. Shi, Z. Wang, Microstructure and intermetallic growth effects on shear and fatigue strength of solder joints subjected to thermal cycling aging, Mater. Sci. Engin. 307 (1) (2001) 42–50.
[101] N. Park, C. Han, D. Kim, Effect of moisture condensation on long-term reliability of crystalline silicon photovoltaic modules, Microelectron. Reliab. 53 (12) (2013) 1922–1926, doi:10.1016/j.microrel.2013.05.004.
[102] C. Peike, S. Hoffmann, P. Hülsmann, B. Thaidigsmann, K.A. Wei$\beta$, M. Koehl, P. Bentz, Origin of damp-heat induced cell degradation, Solar Energy Mater. Solar Cells 116 (2013) 49–54, doi:10.1016/j.solmat.2013.03.022.
[103] S. Pingel, Y. Zemen, O. Frank, T. Geipel, J. Berghold, Mechanical stability of solar cells within solar panels, in: Proceedings of the 24th EUPVSEC, Dresden, Germany, WIP, 2009, pp. 3459–3464.
[104] S. Pingel, Y. Zemen, O. Frank, T. Geipel, J. Berghold, Mechanical stability of solar cells within solar panels, in: Proc. of 24th EUPVSEC, 2009, pp. 3459–3464.
[105] D. Polverini, M. Field, E. Dunlop, W. Zaaiman, Polycrystalline silicon pv modules performance and degradation over 20 years, Progr. Photovolt. 21 (5) (2013) 1004–1015, doi:10.1002/pip.2197.
[106] K. Prakash, T. Sritharan, Interface reaction between copper and molten tin–lead solders, Acta Mater. 49 (13) (2001) 2481–2489.
[107] R.E. Pratt, E.I. Stromswold, D.J. Quesnel, Mode i fracture toughness testing of eutectic sn-pb solder joints, J. Electron. Mater. 23 (4) (1994) 375–381.
[108] P. Protsenko, A. Terlain, V. Traskine, N. Eustathopoulos, The role of intermetallics in wetting in metallic systems, Scr. Mater. 45 (12) (2001) 1439–1445.
[109] pveducation. (Accessed: 2017 January 10). Http://www.Pveducation.Org/pvcdrom/design/metal-grid-pattern.
[110] A. Raga, K.. Carlson, Selective soldering by laser Accessed: 2017 January 17, 2011 *http://www.us-tech.com/Relld/.../selective_soldering_by_laser.htm*.
[111] F. Reil, A. Sepanski, W. Herrmann, J. Althaus, W. Vaaßen, H. Schmidt, Qualification of arcing risks in pv modules, Paper presented at the Photovoltaic Specialists Conference (PVSC), 2012 38th IEEE, 2012.
[112] REN21, Ecowas Renewable Energy and Energy Efficiency - Status Report, 2014 Retrieved from Paris.
[113] Rubin, L., & Schneider, A. Interconnection technology for conventional and concentrator modules (solar cells). Paper Presented at the LEOS 2007-IEEE Lasers and Electro-Optics Society Annual Meeting Conference Proceedings.
[114] L. Rubin, A. Schneider, Interconnection technology for conventional and concentrator modules (solar cells), Paper presented at the Lasers and Electro-Optics Society, 2007. LEOS 2007. The 20th Annual Meeting of the IEEE, 2007.
[115] S. Kluska, F. G., M. Hermle, S.W. Glunz, Loss analysis of high-efficiency back-contact back-junction silicon solar cells, Paper presented at the 23rd European Photovoltaic Solar Energy Conference and Exhibition, 1-5 September 2008, 2008.
[116] T. Saga, Advances in crystalline silicon solar cell technology for industrial mass production, NPG Asia Mater. 2 (3) (2010) 96–102.
[117] H. Sai, T. Matsui, Challenges and prospects of very thin ($< 50$ $\mu$m) crystalline silicon solar cells, Paper presented at the 2019 26th International Workshop on Active-Matrix Flatpanel Displays and Devices (AM-FPD), 2019.
[118] H. Sai, T. Oku, Y. Sato, M. Tanabe, T. Matsui, K. Matsubara, Potential of very thin and high-efficiency silicon heterojunction solar cells, Progr. Photovolt. 27 (12) (2019) 1061–1070.
[119] N.S. Sangaj, V. Malshe, Permeability of polymers in protective organic coatings, Progr. Organ. Coat. 50 (1) (2004) 28–39.
[120] P. Sathyanarayana, R. Ballal, L.S. PS, G. Kumar, Effect of shading on the performance of solar pv panel, Energy Power 5 (1A) (2015) 1–4.
[121] H. Schmidhuber, S. Klappert, J. Stollhof, G. Erfurt, M. Eberspächer, R. Preu, Laser soldering–a technology for better contacts, in: Paper Presented at the Proceedings of the 20th European Photovoltaic Solar Energy Conference, Barcelona, Spain, 2005.
[122] F. Schmitt, A. Priessner, B. Kramer, A. Gillner, Application report-laser joining photovoltaic modules-with new laser sources and integrated process control systems, optimized thermal management of the interconnection process can be provided, Ind. Laser Solut. Manuf. 23 (6) (2008) 20.
[123] E.J. Schneller, R.P. Brooker, N.S. Shiradkar, M.P. Rodgers, N.G. Dhere, K.O. Davis, …, W.V. Schoenfeld, Manufacturing metrology for C-Si module reliability and durability part III: module manufacturing, Renew. Sustain. Energy Rev. 59 (2016) 992–1016, doi:10.1016/j.rser.2015.12.215.

[124] A. Schonecker, D. Eikelboom, P. Manshanden, M. Goris, P. Wyers, S. Roberts, …, A. Kress, Ace designs: the beauty of rear contact solar cells, Paper presented at the Photovoltaic Specialists Conference, 2002. Conference Record of the Twenty-Ninth IEEE, 2002.
[125] H. Schulte-Huxel, S. Blankemeyer, A. Merkle, V. Steckenreiter, S. Kajari-Schröder, R. Brendel, Interconnection of busbar-free back contacted solar cells by laser welding, Progr. Photovolt. 23 (8) (2015) 1057–1065.
[126] B. Sørensen, G. Watt, Trends in Photovoltaic Applications, Survey Report of Selected IEA Countries between 1992 and 2005, 2006.
[127] K. Taira, I. Inagawa, S. Imoto, J. Nakata, Proprietary sphelar® technology for sustainable living in the 21st century, Proc. ECOpole 2 (1) (2008) 141–146.
[128] G.M. Tamizhmani, D. Jordan, H. Gopalakrishna, A. Sinha, A. Balasubramaniyan, J. Oh, K. Dolia, Correlation of Qualification and Accelerated Testing with Field Degradation, 2019 Retrieved from.
[129] B. Thaidigsmann, J. Greulich, E. Lohmüller, S. Schmeißer, F. Clement, A. Wolf, …, R. Preu, Loss analysis and efficiency potential of p-type mwt–perc solar cells, Solar Energy Mater. Solar Cells 106 (2012) 89–94.
[130] J.K. Tien, B.C. Hendrix, A.I. Attarwala, Creep-fatigue interactions in solders, Comp. Hybrids Manuf. Technol. IEEE Trans. 12 (4) (1989) 502–505, doi:10.1109/33.49007.
[131] A.K. Tossa, Y. Soro, L. Thiaw, Y. Azoumah, L. Sicot, D. Yamegueu, …, G. Razongles, Energy performance of different silicon photovoltaic technologies under hot and harsh climate, Energy 103 (2016) 261–270.
[132] J. Tracy, N. Bosco, F. Novoa, R. Dauskardt, Encapsulation and backsheet adhesion metrology for photovoltaic modules, Progr. Photovolt. 25 (1) (2017) 87–96.
[133] J. Tracy, D. D'hooge, N. Bosco, R. Dauskardt, Framework for modelling interface degradation in photovoltaic modules at the molecular level, Paper presented at the 2018 IEEE 7th World Conference on Photovoltaic Energy Conversion (WCPEC)(A Joint Conference of 45th IEEE PVSC, 28th PVSEC & 34th EU PVSEC), 2018.
[134] K. Tu, R. Thompson, Kinetics of interfacial reaction in bimetallic cu sn thin films, Acta Metallurgica 30 (5) (1982) 947–952.
[135] UL1703, Standards for safety, Flat-Plate Photovoltaic Modules and Panels, 1703, Underwriters Laboratories, Northbrook, Illinois, USA, 1993.
[136] E.E. van Dyk, E.L. Meyer, Analysis of the effect of parasitic resistances on the performance of photovoltaic modules, Renew. Energy 29 (3) (2004) 333–344, doi:10.1016/S0960-1481(03)00250-7.
[137] Weber, K., Everett, V., MacDonald, J., Blakers, A. W., Deenapanray, P., & Babaei, J. (2004). Modelling of silver modules incorporating a lambertian rear reflector.
[138] A.W. Weeber, R. Kinderman, C.J.J. Tool, F. Granek, P.c.D. Jong, How to achieve 17% cell efficiencies on large back-contacted mc-Si solar cells, Paper presented at the Photovoltaic Energy Conversion, Conference Record of the 2006 IEEE 4th World Conference on, 2006.
[139] S.R. Wenham, M.A. Green, M.E. Watt, Applied Photovoltaics, Center for Photovoltaic Devices and Systems, University of New South Wales, Sydney, Australia, 1994.
[140] S. Wiese, R. Meier, F. Kraemer, Mechanical behaviour and fatigue of copper ribbons used as solar cell interconnectors, Paper presented at the Thermal, Mechanical & Multi-Physics Simulation, and Experiments in Microelectronics and Microsystems (EuroSimE), 2010 11th International Conference on, 2010.
[141] M. Wiesenfarth, T. S., J. Jaus, F. Eltermann, M. Passig, A.W. Bett, Investigation on interconnection technology for cpv systems, in: Paper presented at the Proceedings from 25th European PV Energy Conference and Exhibition, Valencia, Spain, 2010.
[142] wikipedia. (2017). Https://en.Wikipedia.Org/wiki/reflow_soldering.
[143] H. Wirth, Lasers in wafer-based pv module production, Laser Tech. J. 7 (4) (2010) 36–38, doi:10.1002/latj.201090057.
[144] W.-Q. Wu, D. Chen, R.A. Caruso, Y.-B. Cheng, Recent progress in hybrid perovskite solar cells based on n-type materials, J. Mater. Chem. A 5 (21) (2017) 10092–10109.
[145] M.T. Zarmai, N.N. Ekere, C.F. Oduoza, E.H. Amalu, A review of interconnection technologies for improved crystalline silicon solar cell photovoltaic module assembly, Appl. Energy 154 (2015) 173–182, doi:10.1016/j.apenergy.2015.04.120.
[146] J. Zhao, A. Wang, P. Campbell, A 19.8% efficient honeycomb multicrystalline silicon solar cell with improved light trapping, IEEE Trans. Electron Devices 46 (10) (1999) 1978–1983, doi:10.1109/16.791985.